Doctoral Dissertations

Student Theses and Dissertations

Fall 2010

HAART drugs induce oxidative stress and mitochondrial dysfunction in blood-brain barrier

Kalyan Reddy Manda

Recommended Citation

HAART DRUGS INDUCE OXIDATIVE STRESS AND MITOCHONDRIAL

DYSFUNCTION IN BLOOD-BRAIN BARRIER

by

MANDA KALYAN CHAKRAVARTHY REDDY

A DISSERTATION

Presented to the Faculty of the Graduate School of the

MISSOURI UNIVERSITY OF SCIENCE AND TECHNOLOGY

In Partial Fulfillment of the Requirements for the Degree

DOCTOR OF PHILOSOPHY

in

CHEMISTRY

2010

Approved by

Nuran Ercal, Advisor
Philip Whitefield
Ekkehard Sinn
Melanie R. Mormile
Katie B. Shannon

ABSTRACT

The era of highly active antiretroviral therapy (HAART) has controlled AIDS and its related disorders considerably; however, the prevalence of HIV-1-associated neurocognitive disorders (HAND) has been on the rise in the post-HAART era. In view of these developments, we investigated whether a HAART drug combination of 3'-Azido-2', 3'-deoxythymidine (AZT) and Indinavir (IDV) can alter the functionality of the blood-brain barrier (BBB) endothelial cells, thereby exacerbating the condition. Viability of hCMEC/D3 cells (*in vitro* model of BBB) that were exposed to the drugs was significantly reduced after a 72 hr treatment, in a dose-dependent manner. Reactive oxygen species (ROS) were highly elevated after the exposure, indicating that mechanisms that induce oxidative stress were involved. Measures of oxidative stress such as glutathione (GSH) and malondialdehyde (MDA) were found to be altered in the treated groups. Loss of mitochondrial membrane potential ($\Delta\Psi_m$) assessed with fluorescent microscopy and decreased levels of ATP indicated that cytoxicity was mediated through mitochondrial dysfunction. Furthermore, AZT + IDV treatment caused apoptosis in endothelial cells as assessed by the expression of cytochrome *c* and procaspase-3 proteins. *In vivo* experiments with HIV-1 transgenic animal treated with AZT+IDV showed decrease in GSH in the BBB and brain and increase in MDA levels in the BBB. Thiol antioxidant N-acetylcysteine amide (NACA) reversed some of the pro-oxidant effects of AZT+IDV in both *invitro* and *invivo* studies.

Results from our studies indicate that the AZT + IDV combination can affect the BBB and may play a role in contributing to neurocognitive disorders in HIV-1 infected individuals treated with HAART drugs.

ACKNOWLEDGMENTS

To say that I took my time in the preparation of this dissertation would be an understatement. At the outset, therefore, I thank those mentioned below most of all for their indulgence and patience with my somewhat intermittent work ethic. First and foremost, I owe my deepest gratitude to my advisor Dr. Nuran Ercal, for her constant support and encouragement during the course of pursuing my PhD. This dissertation would not have been possible without her guidance and moral support from point of time when achieving a PhD appeared to be an insurmountable task. She showed me different ways to approach a research problem and the need to be persistent to accomplish any goals. I extend my thanks to my committee members, Dr. Whitefield, Dr. Sinn, Dr. Mormile and Dr. Shannon for their time and support. Special thanks are due to Barbara Harris for her careful correction of manuscripts and other written material.

I would like to thank my entire former and current lab members for making the lab work an inspiring experience of perseverance. I would like to express my deepest gratitude to all of my friends, Swathi, Sashidhar, Hari, Kishore, and every one of those who have always supported me through tough times. I would like to express my thanks and respects my late father Pushkar Reddy for his never ending motivation at every step of life. Thanks are due to my mother Subhashini, brother Bapi, and my sisters, for their love and their support while pursuing my endeavors. I thank God for always being there for me and leading me. Last, but not least, none of this would have been possible without Aruna, my partner, friend, advisor, strength, and biggest reason for my coming this far.

TABLE OF CONTENTS

LIST OF ILLUSTRATIONS

LIST OF TABLES

NOMENCLATURE

ART   Antiretroviral Therapy

AZT   3'-Azido-2', 3'-deoxythymidine

BBB   Blood-Brain Barrier

BM   Basement Membrane

CAT   Catalase

gp120   HIV-1 Envelope Glycoprotein 120

GSH   Glutathione

HIV-1   Human Immunodeficiency Virus

HAND   HIV-1- Associated Neurocognitive Disorders

HAART   Highly Active Antiretroviral Therapy

IDV   Indinavir

MDA   Malondialdehyde

NO   Nitric Oxide

PC   Pericytes

PI   Protease Inhibitors

PUFAs   Polyunsaturated Fatty Acids

Tat   Transregulatory Protein

TJ   Tight Junctions

ROS   Reactive Oxygen Species

SIV   Simian Immunodeficiency Virus

SOD   Superoxide Dismutase

1. INTRODUCTION

Human immunodeficiency virus type 1 (HIV-1) is a lentivirus (a member of the retrovirus family) that causes acquired immunodeficiency syndrome (AIDS), a condition in humans in which the immune system begins to fail, leading to life-threatening opportunistic infections. HIV-1 infection has also been identified for its ability to target the nervous tissues. Infection of the nervous system with HIV can lead to a syndrome of neurological dysfunction currently termed as HIV-associated neurocognitive disorders; HAND (Antinori et al., 2007). HAND is a collective term used to denote the neurological complications of AIDS, consisting of the triad of cognitive, behavior, and motor dysfunction (McArthur et al., 2004). HAND develops in about one third of patients who progress to AIDS. The precise mechanisms of pathogenesis involved in HIV induced central nervous system injury are still not completely understood.

The blood- brain barrier (BBB), a selective interface between blood and the central nervous system, regulates the transport of substances from blood to brain and brain to blood (Banks et al., 2005). The disruption of this layer has been implicated in number of neurocognitive disorders like Alzheimer's and Parkinson's disease (Zipser et al., 2007; Power et al., 1993). A mild to normal grade disruption has been found in HIV patients with neurocognitive disorders (Power et al., 1993). Recent studies have reported that viral proteins like glyco-protein 120 (gp 120) and transregulatory (Tat) protein can alter the endothelial function and disrupt the blood brain barrier, both *in vitro* and *in vivo,* through an oxidative stress mediated mechanism (Price et al., 2006, Banerjee et. al.,

2010). These alterations can play critical roles in the signaling pathways that lead to upregulation of inflammatory genes in the BBB and accelerate neurodegeneration.

Introduction of highly active antiretroviral therapy (HAART), the combination of two or more classes of antiretroviral drugs, has led to a considerable decline in HIV disease progression rates and related opportunistic infections. Despite these significant improvements in health conditions, mild cognitive impairment in HIV -infected individuals seems to be on the rise and still remains a public health concern in the HAART era (Sacktor et al., 2002). Recent studies have shown that neurocognition improved significantly following discontinuation of HAART in subjects with preserved immune function (Robertson et al., 2010). HAART regimens have been recognized as leading to mitochondrial toxicity and are associated with cardiac, hepatic, hematologic, and myopathic morbidity (Carr et al., 1999). Numerous mechanisms have been proposed to explain the deleterious impact of HAART drugs, including mitochondrial DNA depletion, impaired mitochondrial replication via inhibition of the mitochondrial DNA polymerase gamma (POLγ), and subsequent increase in reactive oxygen species and oxidative stress (Lewis et al., 2003).

The above discussed research, concerning the effects of HAART drugs in various metabolic disorders raises doubt about the possible impact of antiretroviral therapy on the BBB and neurocognition in HAART-treated HIV patients. To the best of our knowledge, no known study has been done to evaluate the effect of HAART drugs on the human blood-brain barrier and the mechanism involved in this effect. In order to address this concern, we hypothesized that HAART drugs may cause endothelial dysfunction in the BBB, thereby exacerbating HIV-1- associated neurocognitive disorders. In order to

test our hypothesis we evaluated the effect of the combination of 3'-Azido-2', 3'-deoxythymidine (AZT), and Indinavir (IDV), (a commonly recommended HAART regimen) on various oxidative stress parameters, as well mitochondrial dysfunction in blood-brain barrier endothelial cells (Yeni et al., 2004). In addition to this, toxicity of HIV proteins, HAART toxicity appears to be related through a common phenomenon of oxidative stress. The possible involvement of oxidative stress suggests the use of antioxidants in suppressing harmful effects and protecting the BBB. Recently, a new low molecular thiol antioxidant, N-acetylcysteine amide (NACA), with the ability to cross the BBB has been effective in protecting cells from viral proteins in *in vitro* and *in vivo* studies in our lab (Price et.al., 2006). So we investigated the role of oxidative stress in viral proteins and HAART drugs induced toxicity in the BBB of HIV-1 transgenic mice. Concomitantly, we explored the antioxidant effect of NACA in reversing the oxidative stress related effects induced by viral proteins and HAART drugs on the BBB.

2. REVIEW OF LITERATURE

2.1. GLOBAL STATISTICS ON HIV

In 1981, the first cases of acquired immunodeficiency syndrome (AIDS) were reported to the Centers for Disease Control and Prevention (CDC). Since that time, the HIV epidemic has expanded to become one of the greatest public health challenges, both nationally and globally. There are estimated to be around 33.2 million people living with HIV or AIDS worldwide today and around 2.5 million more people are newly infected with HIV every year. Of the 2.5 million people newly infected with HIV each year, 50% of them are under the age of 25 years. Around 22.5 million people who are currently infected with HIV or AIDS are living in Africa, and more than one million people were living with AIDS in USA. A total of 25 million people have died from AIDS since the year 1981 and it is estimated that more than half a million have died in the U.S alone (Woods et al., 2009).

2.2. STRUCTURE OF HIV

HIV is an enveloped RNA virus whose basic structure consists of an outer bilayer of lipid and glycoprotein and an inner core containing two single RNA strands bound together by a *gag*-derived protein, p24. The outer membrane of HIV contains specific structural elements that play important roles in infectivity and disease progression. The most important of these is the viral envelope glycoprotein 120 (gp120), which is necessary for HIV's interaction with host cell receptors on cells, including CD4+ lymphocytes, macrophages, and monocytes. Gp120 is closely associated with the envelope transmembrane viral protein, gp41, which is involved in viral–cell membrane

fusion. Both gp41 and gp120 are essential for infectivity. Gp120 interacts with the CD4+ receptor on the surface of susceptible cells. However, gp120 attachment also requires the presence of chemokine co-receptors, such as CXCR4 or CCR5, which facilitate the process of cell binding and entry (Gonda, 1988).

2.3. HIV-1-ASSOCIATED NEUROCOGNTIVE DISORDERS (HAND)

HIV enters the CNS early in the course of infection, and the virus resides primarily in microglia and macrophages. However, infection of these cells may not be sufficient to initiate neurodegeneration (Gartner et al., 2000). It has been proposed that factors associated with advanced HIV infection in the periphery (non-CNS) are important triggers for events leading to neurocognitive disorders (Kaul et al., 2001). The clinical manifestations of CNS disorders in HIV/AIDS include depression and all degrees of cognitive impairment collectively termed as HIV-1-associated neurocognitive disorder (HAND). HAND is characterized by a triad of cognitive, behavioral, and motor dysfunctions (McArthur, 2004). For milder forms of HAND, difficulties in concentration, attention, and memory may be present although the neurologic examination is unremarkable. Affected individuals are easily distracted, lose their train of thought, and require repeated prompting. Activities of daily living may take longer and become more laborious.

More severe forms of HAND, such as HIV- associated dementia, are seen in untreated HIV individuals. Cognitive and motor dysfunctions are more pronounced in these individuals, and the assistance of a caregiver is required to maintain activities of daily living. The most commonly observed symptoms include delayed speech output with long pauses between words, poor thought and emotional content characterized by lack of

spontaneity, and social withdrawal that is often mistakenly diagnosed as severe

depression. Gait abnormalities and a reduction in motor movements are observed (Woods

et al., 2009).

To date, the four possible mechanisms that are supportive of viral entry into the

CNS and are currently under investigation include: the transmission of virus in infected

macrophages (the Trojan horse model), direct infection of the blood-brain barrier (BBB)

by HIV; transcytosis of HIV; and BBB disruption (Piacentini et al., 2005). This neuro

invasion in turn elicits a series of neuroinflammatory responses, resulting in neurologic

dysfunctions in a significant number of individuals with AIDS. This is characterized by

BBB disruption, leukocyte infiltration into the CNS, formation of microglia nodules and

multinucleated giant cells, astrocyte activation and eventual damage and/or loss of

neurons (Xu et al., 2005). To date the mechanisms leading to HAND in AIDS patients are

not fully understood; however, it is thought that activated macrophage, microglia, and

astrocytes produce chemokines and cytokines that in conjunction with secreted viral

proteins may damage the BBB and leading to increased permeability and neuronal

demise (Giulian et al., 1990; Bellizzi et al., 2006; Rumbaugh and Nath, 2006).

2.4. BLOOD-BRAIN BARRIER

The BBB is crucial in HIV infection of the CNS (Gartener et al., 2000). The BBB

is an endothelial barrier present in capillaries that innervate the brain. The BBB is

selective barrier which impedes entry from the blood to the brain of virtually all

molecules, except those that are small and lipophilic. The BBB endothelial cells differ

from endothelial cells in the rest of the body by the absence of fenestrations, more

extensive tight junctions (TJs), and sparse pinocytic vesicular transport. Endothelial cell

tight junctions limit the paracellular flux of hydrophilic molecules across the BBB. In contrast, small lipophilic substances such as O_2 and CO_2 diffuse freely across plasma membranes along their concentration gradient (Grieb et al., 1985). Nutrients including glucose and amino acids enter the brain via transporters, whereas receptor-mediated endocytosis mediates the uptake of larger molecules including insulin, leptin, and iron transferrin (Pardridge et al., 1985; Zhang et al., 2001). In addition to endothelial cells, the BBB is composed of the capillary basement membrane (BM), astrocyte end-feet ensheathing the vessels and pericytes (PCs) embedded within the BM. The TJ consists of three integral membrane proteins, namely, claudin, occludin, and junction adhesion molecules, and a number of cytoplasmic accessory proteins including ZO-1, ZO-2, ZO-3, cingulin, and others. Claudins-1 and -2 are 22 kDa phosphoprotein and have four transmembrane domains. Claudins bind to claudins on adjacent endothelial cells to form a primary seal of the TJ (Furuse et al., 1999). A carboxy terminal of claudins binds to cytoplasmic proteins including ZO-1, ZO-2, and ZO-3. Occludin is a 65-kDa phosphoprotein, significantly larger than claudin. Occludin has four transmembrane domains, a long COOH-terminal cytoplasmic domain, and a short NH_2-terminal cytoplasmic domain. The two extracellular loops of occludin and claudin, originating from neighboring cells, form the paracellular barrier of TJ. The cytoplasmic domain of occludin is directly associated with ZO protein. Cytoplasmic proteins involved in TJ formation include zonula occludens proteins (ZO-1, ZO-2, and ZO-3), cingulin, 7H6, and several others. Importantly, actin, the primary cytoskeleton protein, binds to COOH-terminal of ZO-1 and ZO-2, and this complex cross-links transmembrane elements and thus provides structural support to the endothelial cells. In pathologic conditions, a

number of chemical mediators are released that increase BBB permeability. Several of these mediators of BBB opening have been studied in both *in vivo* and *in vitro* experiments and include glutamate, aspartate, taurine, ATP, endothelin-1, NO, MIP-2, tumor necrosis factor-a (TNF-α), and IL-β, which are produced by astrocytes . Other agents reported to increase BBB permeability are bradykinin, 5HT, histamine, thrombin, UTP, UMP, substance P, quinolinic acid, platelet activating factor, and free radicals (Abbott, 2002; Annunziata et al., 1998; Pan et al., 2001; Stastny et al., 2000).
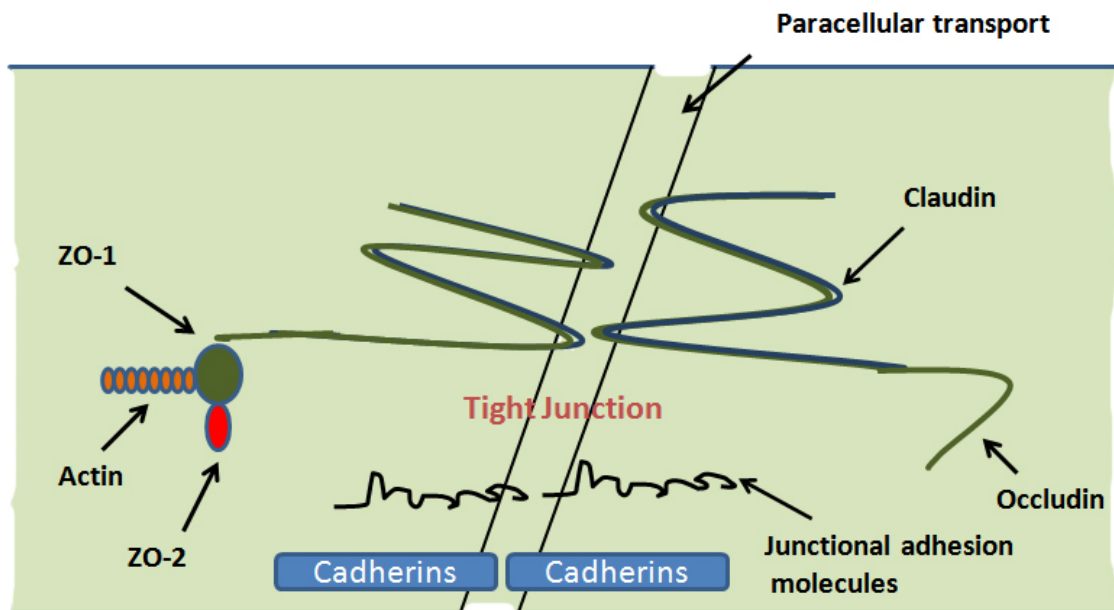
Figure 2.1. Schematic representation of protein interactions at tight junctions

Histological studies of specimens from HIV-1-infected humans and simian immunodeficiency virus (SIV)-infected rhesus macaques show that lymphocytes and monocytes migrate into the brain (Prospero-Garcia et al., 1996; Kalams et.al., 1995).

However, the relevance of CNS-invading lymphocytes in HAND is not clear. It has also been suggested that the inflammatory cytokine tumour-necrosis factor-a (TNF-) opens a paracellular route for HIV-1 across the BBB (Fiala et al., 1997). These findings indicate that one reason why HAND rarely occurs before the onset of advanced HIV disease is that a scathing cycle of immune dysregulation and BBB dysfunction is required to achieve sufficient entry of infected or activated immune cells into the brain to cause neuronal injury. Alterations of the BBB have been observed in transgenic mice expressing the HIV envelope protein gp120 in a form that circulates in plasma, suggesting that circulating virus or envelope proteins may also cause BBB dysfunction during the viremic phase of primary infection (Toneatto et al., 1999).

2.5. OXIDATIVE STRESS IN BBB DYSFUNCTION

Free radicals are compounds possessing an unpaired electron, which renders them highly reactive and capable of causing oxidative damage to all the major macro-molecules in cells, including lipids, proteins and nucleic acids (Zoccal et al., 2000). A major family of free radicals is the reactive oxygen species (ROS), derived metabolically from molecular oxygen via superoxide anions (O_2^-). Oxidative attack on proteins results in the formation of protein carbonyls, often with the loss of functionality of the parent protein. Polyunsaturated fatty acids, which are major components of cell membranes, can also undergo free radical attack, producing lipid peroxidation products like malondialdehyde (MDA) and 4-hydroxynonenal (Halliwell et al., 1997). Under normal circumstances, the body is protected from such damage by a careful balance between pro-oxidants and cellular antioxidants like glutathione. Any imbalance between the pro-oxidants and antioxidants results in a condition called oxidative stress.

Under physiological conditions, the integrity of the BBB is shielded from oxidative stress because the brain endothelial cells have high cellular levels of antioxidants such as GSH, superoxide dismutase (SOD), catalase (CAT) and glutathione peroxidase (GPx). These enzymes protect the cells from free radicals and peroxidative damage (Price et al., 2006). On the other hand, BBB is highly susceptible to oxidative damage due to the presence of poly unsaturated fatty acids (PUFA's). These fatty acids are easily peroxidizable leading to lipid peroxidation metabolites like MDA. Free radical production and the resulting oxidative stress, along with circulating inflammatory chemokines, play a key role in HAND (Agarwal et. al., 1999).

Viral proteins, gp 120 and Tat have been shown to cause oxidative stress in endothelial cells. The mechanism by which HIV-1 proteins induce oxidative stress is not completely known. One proposed mechanism is that HIV-1 induced neurotoxicity may be due to an increased production of ROS by HIV-1 proteins (gp120 and Tat). The pathogenesis of HIV-1 infection has implicated increased levels of ROS. HIV-infected individuals have abnormally low levels of antioxidants, such as glutathione (GSH), the major intracellular defense against the production of ROS. Additionally, a reduction in GSH levels, accompanied by elevated levels of malondialdehyde (MDA), a reflection of increased levels of lipid peroxidation, has been reported in HIV-1 infected patients (Sonneberg et al., 1988).

The HIV-1 envelope glycoprotein (gp120) and transregulatory protein (Tat) of HIV-1 are neurotoxic and cytotoxic and have been implicated in the development of HAND. They are known to cause oxidative stress and have been associated with disruption of the BBB (Annuziata et al., 2003). Recently, it has been shown that there is

some evidence that binding of gp120 or Tat protein to brain endothelial cells may cause

many of the changes seen in the BBB. For example, one study found a significant

increase in permeability (up to 47%) in cultured endothelial cells after exposure to gp120

(Cioni et al., 2002). Another study confirmed that gp120 is capable of changing and

activating the vascular component of the BBB *in vivo* (Tonneato et al., 1999). Another

study of HIV-1 Tat protein demonstrated that exposure of endothelial cells to HIV-1 Tat

protein resulted in a dose-dependent increase in oxidative stress and a decrease in

intracellular GSH (Toborek et al., 2003). GSH, which is an important intracellular non-

protein thiol compound in the mammalian cells, has a pivotal role in the maintenance of

membrane integrity. It may also play an important role in the proper functioning of the

BBB (Agarwal et. al., 1999). Although brain endothelial cells possess high intracellular

levels of antioxidative defense mechanisms, such as GSH, GSH peroxidase, and catalase,

exposure to toxins and drugs may render the BBB susceptible to toxic damage and alter

its specific functions.

Both gp120 and Tat are able to induce apoptosis of cultured neurons and can

render neurons vulnerable to excitoxicity and oxidative stress (Corasaniti et al, 2001).

Other viral proteins, Nef, Vpr, and protease, are also suggested as sources of oxidative

stress, as well as being disruptive and causing change in the mitochondrial

transmembrane potential (Aksenova et al., 2005). Most researchers believe that the least

instigation of apoptosis by oxidative stress is during HAND, although other factors may

also play key or supportive roles. Pro-apoptotic conditions related to oxidative stress

include: depletion of Bcl-2, (an anti-apoptotic/antioxidant protein), decrease in apoptosis

in cells infected with HIV (even though antioxidants are provided), and secretion of pro-

apoptotic/pro-oxidant cytokines (molecular signalers) from macrophages (Lipton et al., 1995)

It has been found that the death of neurons in a rat cortex neuronal culture, mediated by gp120, was due to nitric oxide (NO) production (Dawson et al., 1993). NO, which is synthesized by vascular endothelial cells, is a very strong vasodilatory substance. NO also helps to modulate signaling in intercellular and intracellular communication for BBB permeability. In addition, NO regulates ion channels in cells, neurotransmissions, and cytotoxicity. NO may not be the only toxin, or even the only free radical, associated with HAND. Vague schematics of general pathways for infection are proposed, however. It is commonly thought that gp120 plays a role in the infection of the BBB's endothelial cells, creating an environment in which there is greater nitric oxide synthase (NOS) production. Once the NOS produces more NO, the NO could cause the breakdown of the BBB's endothelial cells, rendering it ineffective in its usual functions (Dawson et al., 1993). Previous research has also demonstrated that oxidative stress was induced in brain endothelial cells *in vitro* and *in vivo*, when exposed to the HIV-1 proteins gp 120 and Tat protein depleted intracellular GSH, increased lipid peroxidation, and reduced antioxidant enzyme levels (catalase, GPx, glutathione reductase). CD-1 mice, injected with these proteins (gp120 + Tat) also decreased the expression of tight junction proteins ZO-1, ZO-2, Occludin, and Claudin-5 (Banerjee et al., 2010).

2.6. HIGHLY ACTIVE ANTIRETROVIRAL THERAPY (HAART)

During the last twenty years, major progress has been made in the understanding and treatment of human immunodeficiency virus (HIV) infection. Different classes of antiretroviral agents are approved for the treatment of HIV-infection (Table 2.1). These

substances could be divided into three classes, based on their mechanisms of action (Clercq et al., 2005).

Reverse transcriptase inhibitors (RTIs): This class of drugs targets construction of viral DNA by inhibiting activity of reverse transcriptase. There are two subtypes of RTIs with different mechanisms of action: nucleoside-analogue RTIs (NRTIs) are incorporated into the viral DNA leading to chain termination, while non-nucleoside-analogue RTIs (NNRTIs) distort the binding potential of the reverse transcriptase enzyme. RTIs come in three forms:

- Nucleoside analog reverse transcriptase inhibitors (NARTIs or NRTIs)
- Nucleotide analog reverse transcriptase inhibitors (NtARTIs or NtRTIs)
- Non-nucleoside reverse transcriptase inhibitors (NNRTIs)

The mode of action of NRTIs and NtRTIs is essentially the same; they are analogues of the naturally occurring deoxynucleotides needed to synthesize the viral DNA and they compete with the natural deoxynucleotides for incorporation into the growing viral DNA chain. However, unlike the natural deoxynucleotides substrates, NRTIs and NtRTIs lack a 3'-hydroxyl group on the deoxyribose moiety. As a result, following incorporation of an NRTI or an NtRTI, the next incoming deoxynucleotide cannot form the next 5'-3' phosphodiester bond needed to extend the DNA chain. Thus, when an NRTI or NtRTI is incorporated, viral DNA synthesis is halted, a process known as chain termination (Jochmans et al., 2008). All NRTIs and NtRTIs are classified as competitive substrate inhibitors. In contrast; NNRTIs have a completely different mode of action. NNRTIs block reverse transcriptase by binding at a different site on the

enzyme, compared to NRTIs and NtRTIs. NNRTIs are not incorporated into the viral DNA but instead inhibit the movement of protein domains of reverse transcriptase that are needed to carry out the process of DNA synthesis. NNRTIs are therefore classified as non-competitive inhibitors of reverse transcriptase.

Protease inhibitors (PIs): HIV-1 protease is a complex enzyme composed of two identical halves (ie, a symmetrical dimer) with an active site located at the base of the cleft. It is responsible for the cleavage of the large viral precursor polypeptide chains into smaller, functional proteins, thus allowing maturation of the HIV virion. This process takes place in the final stages of the HIV life cycle. Inhibition of the protease enzyme results in the release of structurally disorganized and noninfectious viral particles. Protease inhibitors target viral assembly by inhibiting the activity of protease, an enzyme used by HIV to cleave nascent proteins for final assembly of new virons. HIV PI's target the peptide linkages in the gag and gag-pol polyproteins which must be cleaved by protease (Monini et al., 2003). All approved PI's contain a hydroxyethylene bond instead of a normal peptide bond. The hydroxyethylene bond makes PI's non-scissile substrate analogs for HIV protease (Figure 2.2). There are 10 PIs currently approved for clinical use. Drug interactions are important considerations with the use of PIs. Protease inhibitors are substrates for the cytochrome P450 system (primarily CYP3A4) and are themselves, to varying degrees, inhibitors of this system, with ritonavir being the most potent inhibitor.

Some PIs, such as lopinavir and tipranavir, are also inducers of CYP3A4. This leads to a significant number of interactions with drugs that are inducers, inhibitors, or substrates of this system (Block et al., 2004).

Fusion inhibitors: These drugs block HIV from fusing with a cell's membrane to enter
and infect it.

Table 2.1. Approved HAART drugs

Protease Inhibitors	NRTIs	NNRTIs	Mixed Class
Mprenavir	Abacavir	Delavirdine	enfuvirtide (fusion inhibitor)
Atazanavir	Didanosine (ddI)	Efavirenz	maraviroc (CCR5 antagonist)
Darunavir	Emtricitabine (FTC)	Etravirine	raltegravir (integrase inhibitor)
Fosamprenavir	Lamivudine (3TC)	Nevirapine	
Indinavir	Stavudine (d4T)	Delavirdine	
Lopinavir/ritonavir	Zidovudine (AZT)		
Nelfinavir	Zalcitabine (ddC)		

Integrase inhibitors: These drugs inhibit the enzyme integrase, which is responsible for
integration of viral DNA into the DNA of the infected cell. There are several integrase
inhibitors currently under clinical trial but none are commercially available.

Current national guidelines for antiretroviral therapy recommend the use of
combinations of different classes of antiretroviral agents. These therapeutic regimes,
called highly active antiretroviral therapy (HAART), usually consist of 2 NRTIs
combined with a PI or a NNRTI (Clercq et al., 2005). Alternative regimes include 3
NRTIs. HAART is now the standard of care for HIV-therapy and has led to substantial
reduction in morbidity and near-complete suppression of HIV-1 replication.
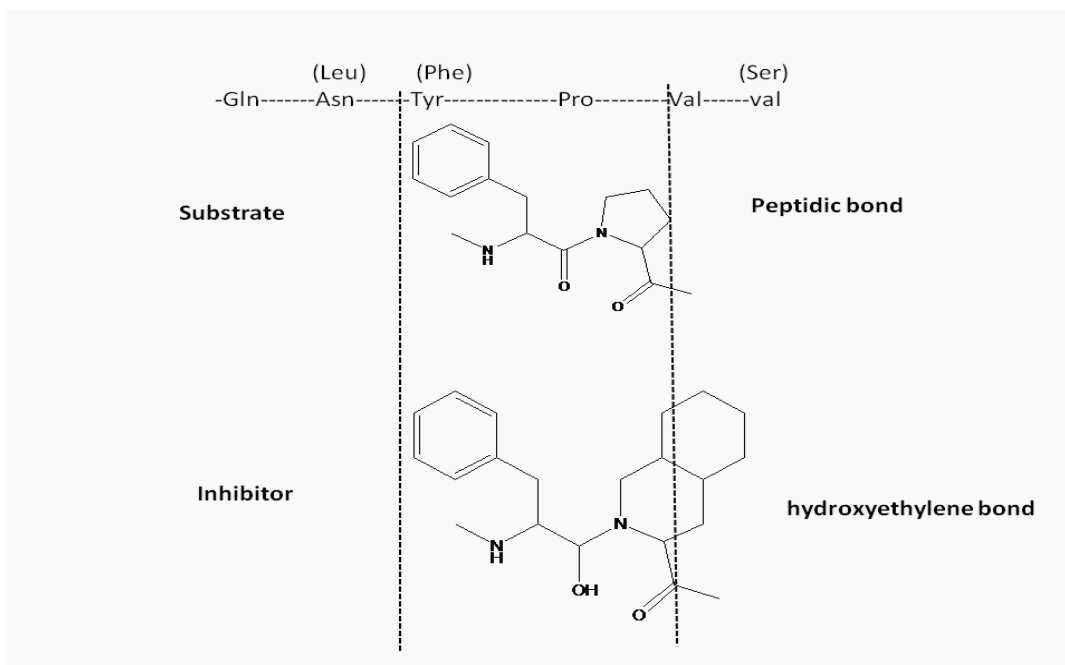
Figure 2.2. Mechanism of action of protease inhibitors.

Since HAART is unlikely to eradicate HIV-1, antiviral therapy may be required for a lifetime, leading to an increase in attention on the long term safety of HAART. Previously, according to the International U.S. AIDS Panel, no known adverse effects have been reported in patients treated with a combination of 3'-azido-2', 3'-deoxythymidine (AZT or Zidovudine), and indinavir (IDV) -one of the most common therapeutic regimens recommended in HAART (Yeni et al., 2004). AZT belongs to the class of NRTIs, and structurally resembles a thymidine (a nucleoside analog) whereas IDV belongs to protease inhibitor family (Figure 2.3). However, several toxicities related to these drugs have been recently reported. As the AZT+IDV combination is one of the common regimens in HAART, our current study was performed utilizing a combination of these drugs to study their effects on BBB endothelial cells.

(A)   **(B)**
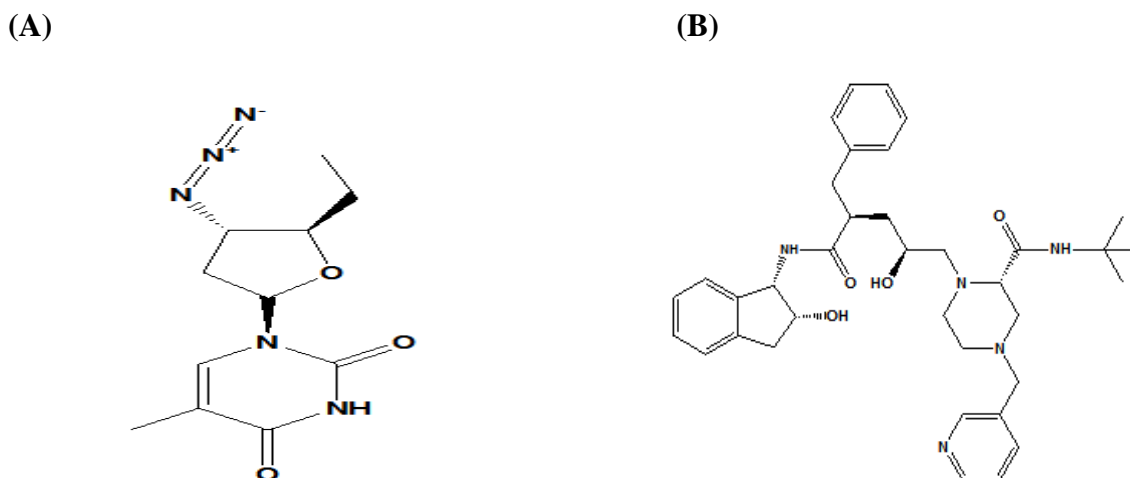
Figure 2.3. Structure of (A) 3'-azido-2', 3'-deoxythymidine (B) Indinavir.

2.7. NEUROCOGNITIVE DISORDERS IN HAART ERA

Since its introduction in 1996, HAART has drastically improved the life

expectancy of those living with HIV. Antiretroviral therapy has led to long-term survival

for HIV-infected individuals. Thus, the number of HIV-infected persons has increased

along with the proportion of those who are considered "older". While the incidence of a

severe form of HAND appears to have decreased since the introduction of HAART, the

prevalence of HAND appears to be on the rise. Unfortunately, it is not at all clear that

HAART provides long-term protection from HAND. In recent years, the incidence of

HAND as an AIDS-defining illness has actually increased and recent studies have

estimated that the prevalence of HAND is unchanged or escalating, even in populations

with extensive use of HAART. The proportion of new cases of HAND demonstrating a

CD4 count greater than 200 is also increasing in HAART patients (Sacktor et al 2001).

The associated toxicity of long-term antiretroviral therapy includes the risk of developing central obesity, dyslipidemia, and insulin resistance (Behrens et al., 1999). It is well known that vascular endothelial dysfunction is a common phenomenon in HAART- treated patients, and this known association between these vascular risk factors and dementia, suggests that long-term HAART use may actually contribute to the risk of acquiring HAND (Whitmer et al. 2005). Metabolic derangement observed in HAART-treated patients that might contribute to HAND risk is the effect of nucleoside reverse transcriptase inhibitors (NRTIs) on mitochondria. HAART regimens that include NRTIs like AZT have been recognized as leading to mitochondrial toxicity and are associated with cardiac, hepatic, hematologic, and myopathic morbidity (Lewis and Dalakas 1995).

Numerous mechanisms have been proposed to explain the deleterious impact of NRTIs, including mitochondrial depletion, impaired mitochondrial replication via inhibition of the mitochondrial DNA polymerase gamma (POLγ), and subsequent increase in ROS (Lewis et al., 2003). POLγ-independent mechanisms of impairing mitochondrial function have also been implicated, including decreased mitochondrial DNA transcription protein glycosylation, and altered expression of lipid metabolism genes (Mallon et al., 2005). Mitochondrial dysfunction is a feature of a number of neurodegenerative diseases, including AD, Parkinson's disease, amyotrophic lateral sclerosis, and Huntington's disease (Knott et al., 2008; Lin and Beal, 2006). Evidence of oxidative stress in the CNS has also been demonstrated in patients with HAND (Turchan et al., 2003). Proton magnetic resonance spectroscopy illustrates mitochondrial dysfunction in patients taking an NRTI as a component of HAART therapy. N-acetylaspartate levels, a marker of neuronal mitochondrial integrity, are lower in frontal

white matter in HIV+ patients taking the NRTIs didanosine or stavudine as compared to those who are HIV- or HIV+ on alternative antiretroviral therapy (Schweinsburg et al. 2005). Additional evidence that NRTI exposure might cause neuronal injury by inducing mitochondrial toxicity comes from an investigation of synaptosomes and brain mitochondria treated with the NRTI, 2′, 3′-dideoxycytidine (ddC). This treatment led to cytochrome *c* release, decreased expression of the antiapoptotic molecule Bcl-2, and increased protein levels of the proapoptotic molecules caspase-3 and Bax, highlighting direct pathways between NRTI therapy and neuronal cell death and dysfunction (Opii et al., 2007)

Another class of drugs primarily involved in HAART treatment includes protease inhibitors like indinavir that have been associated with several toxicities. The deleterious effects of HIV protease inhibitors have been associated with ROS overproduction and also endoplasmic reticulum stress, but the relation between these two events is not known. In human aortic endothelial cells, protease inhibitors alone and as part of HAART regimens increase ROS production (Jiang et al., 2007). Nelfinavir induces oxidative stress and can also lead to adipocyte necrosis (Vincent et al., 2004) and premature senescence in human fibroblasts (Caron et al., 2007). In addition, production of nitric oxide, a mediator of protein nitrosylation, and other ROS that alter cellular redox-dependent reactions interferes with protein disulphide bonding and results in misfolding of proteins that accumulate in endoplasmic reticulum lumen. Treatment of peripheral blood mononuclear cells from healthy donors with a higher concentration (10 μM) of an HIV protease inhibitor, saquinavir or indinavir, has induced both a loss in mitochondrial membrane potential ($\Delta\Psi_m$) and cell death (Estaquier et al., 2002).

Although the exact mechanism still eludes researchers, it is being established that protease inhibitors may have the potential for both beneficial and detrimental effects on human cells independent of their antiretroviral effects.

2.8. ROLE OF N-ACETYLCYSTEINE AMIDE (NACA)

Glutathione (GSH) and other sulfhydryl-containing compounds are found to be decreased in HIV- infected patients' blood, liver, and cerebro spinal fluid samples. Although life expectancy is very poor for these patients, if given GSH, life expectency significantly increases. The roles of GSH in the brain are to protect neurons against ROS and its stable byproducts, such as hydroxynonenal (Pocernich et al., 2005). GSH is also responsible for maintaining redox balance in the brain endothelial cells, thereby protecting them from oxidative stress (Toborek et al., 2005), as well as playing a crucial role in maintaining the BBB's normal functions (Agarwal et al., 1999). As a result, the compounds that increase intracellular GSH such as N-acetylcysteine (NAC), GSH ethyl ester, and GSH, are becoming increasingly popular for treating oxidative stress-related disorders. GSH is the principal intracellular thiol responsible for scavenging ROS and maintaining the oxidative balance in tissues. Cysteine (Cys) and glutathione delivery compounds have been used to protect normal cells from redox imbalance. Therefore, thiol-containing compounds gained special attention due to their profound role in maintaining tissue redox balance. One of the most widely used thiol antioxidants has been NAC (Holdiness et al., 1991). NAC, the drug of choice in acetaminophen (Tylenol) intoxication, indirectly replenished GSH through deacetylation to cysteine, preventing oxidative damage through scavenging of ROS (Cotgreave et al., 1997). It has been shown that it protects cells from radiation-induced damage (Neal et al., 2003).

NAC was suggested as a therapeutic in HIV-1 infected patients, after the

discovery of its effect on the inhibition of virus replication in lymphocytes (Staal et al.,

1990). HIV-1 infected patients showed a decrease in GSH and Cys levels; therefore, it

seemed to be a logical solution to replenish GSH and Cys by NAC (Droge et al., 1992).

Oral NAC increased the intracellular GSH levels, decreased the mortality rate of patients,

and prevented the loss of CD4$^+$ T cells. Recently, NAC analogs have been introduced as

an additional regimen for the treatment of HIV infection (Oiry et al., 2004). However,

NAC has numerous side effects, including being pro-oxidant, suppressing respiratory

burst, and causing a toxic ammonia accumulation in case of liver problems (Cotgreave et

al., 1997). Moreover, NAC's failure to provide significant antioxidant effects *in vivo*,

may be due to its low solubility and tissue distribution (Atlas et al., 1999). A new strategy

has recently been introduced for improving the pharmacokinetic properties of these

agents. This was achieved by neutralizing the carboxylic group of NAC, which made the

drug more lipophilic and cell-permeating (Figure 2.3B). This compound was shown to

cross the BBB, scavenge free radicals, chelate copper, and attenuate myelin

oligodendrocyte glycoprotein (MOG)-induced experimental autoimmune

encephalomyelitis in a multiple sclerosis mouse model (Offen et al., 2004). Further

evidence of the efficient membrane permeation of NACA was demonstrated in a recent

study which assessed NACA for its antioxidant and protective effects in a model using

human red blood cells (Grinberg et al., 2005). NACA has been used as a potential

neuroprotective drug in an animal model of Parkinson's disease, where it reduces

neurodegeneration and progression of the disease. NACA passes through the BBB and

protects the dopaminergic neurons against ROS in *in vivo* and *in vitro* models (Bahat et

al., 2005). NACA and two other newly synthesized thiols (N-acetyl-gly-cys-amide and

N-acetyl-Cys-Gly-Pro-Cys-amide) eliminate β amyloid-induced oxidative stress and

neurotoxicity *in vitro* (Bartov et al., 2006). It has been suggested that NACA and the

other aforementioned thiols cross the BBB and scavenge the free radicals directly or

indirectly by providing Cys and GSH.

(A)
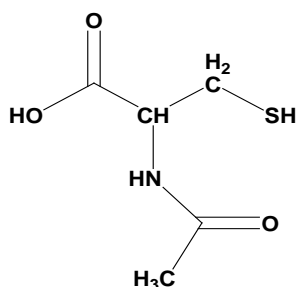
(B)

N-Acetylcysteine (NAC)
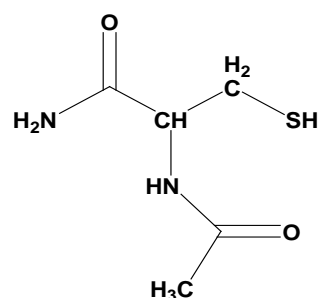
N-Acetylcysteine amide (NACA)

Figure. 2.3. Structures of (A) NAC and (B) NACA. The carboxyl group has been
replaced by amide in NACA.

Recent studies have also investigated the ability of NACA to protect *in vitro* and

in vivo from HIV proteins, diesel exhaust particles that induced oxidative stress, and

toxicity (Banerjee et al., 2010; 2009). Studies from our lab have also reported that NACA

had greater free radical scavenging abilities and reducing powers than NAC (Ates et al.,

2008).

3. EXPERIMENTAL DESIGN

3.1. MATERIALS AND METHODS

3.1.1. Materials. N-(1-pyrenyl)-maleimide (NPM) was purchased from Sigma (St. Louis, MO). N-acetylcysteine amide was provided by Dr. Glenn Goldstein (David Pharmaceuticals, NewYork, NY, USA). High-performance liquid chromatography (HPLC) grade solvents were purchased from Fisher Scientific (Fair Lawn, NJ). AZT and IDV were a gift from the National Institutes of Health AIDS Research and Reference Reagent Program. JC-1 dye (5,5′,6,6′-tetrachloro-1,1′,3,3′-tetraethylben- zimidazolyl carbocyanine iodide) and Fura-2AM were purchased from Invitrogen (San Diego, CA). Calcein AM was purchased from Biotium, Inc, CA. All other chemicals were purchased from Sigma (St. Louis, MO), unless stated otherwise.

3.1.2. Culture of Human Brain Microvascular Endothelial Cells (hCMEC/D3). As an in vitro BBB model, immortalized human brain endothelial cells, hCMEC/D3 (a gift from Dr. Pierre Couraud), were plated on 25 cm2 tissue culture flasks and maintained in EBM-2 medium in humidified 5% CO_2/95% air at 37 °C. The culture medium was changed twice a week and endothelial cells at passages 28–34 were used in this study. A serum-free and growth-factor-free medium was used in the experiments. All assays were performed in triplicate and each experiment was repeated three times. The EBM-2 medium (Lonza, Walkersville, MD), was supplemented with VEGF, IGF-1, EGF, basic FGF, hydrocortisone, ascorbate, gentamycin and 2.5% fetal bovine serum (FBS), as recommended by the manufacturer.

3.1.3. Cytotoxicity Assay.   hCMEC/D3 cells were seeded in a 96-well plate, at

densities of approximately $8x10^3$ cells per well, and were allowed to attach for 24 hr.

The media was then discarded, and the cells were treated with AZT + IDV combination

for 24 hr and 72 hr in a serum-free media. For NACA cytotoxicity studies, the cells were

incubated with various concentrations of NACA for 24 h. Protective effects of NACA

were studied by first preincubating cells with NACA for 1 hr and were treated with

AZT+ IDV for the required time period. After the treatment, the cells were washed three

times with phosphate buffered saline (PBS), and 100 µl of 0.4 µM Calcein AM (Biotium

Inc.) in PBS was added to each well for 30 min at 37 °C. The fluorescence was measured

with an excitation wavelength at 485 nm and an emission wavelength of 530 nm, using a

microplate reader (Fluostar, BMG Labtechnologies, Durham, NC, USA).

3.1.4. Morphological Assessment of hCMEC/D3 cells. Treated hCMEC/D3

cells were assessed for their changes in cellular morphology. An Olympus inverted

microscope (model CKX1SF) with 20X objective was utilized to observe the changes in

their morphology.

3.1.5. Reactive Oxygen Species (ROS) Measurement. Intracellular ROS

generation was measured using a well characterized probe, 2′,7′-dichlorofluorescein

diacetate ($DCFH_2$-DA) (Wang et al., 1999). $DCFH_2$-DA is hydrolyzed by esterases to

dichloro -fluorescein ($DCFH_2$), which is trapped within the cell. This nonfluorescent

molecule is then oxidized to fluorescent dichlorofluorescein (DCF) by the action of

cellular oxidants. The cells were exposed to the drugs for 48 hr. In order to assess the

effect of NACA on ROS levels in 100 µM AZT+IDV treated groups, cells were exposed

to 2 mM of NACA for 1 hr before the treatment. A DCFH$_2$-DA stock solution (in DMSO) of 1mg/ml was diluted in serum-free media to yield a 100 μM working solution. Cells were washed twice with PBS and then incubated with a DCFH2-DA working solution for half an hour in a dark environment (37 °C incubator). The cells were washed with PBS and then fluorescence was measured using a microplate reader.

3.1.6. Determination of Glutathione (GSH) Levels. The level of GSH in the cells was determined by RP-HPLC, according to the method developed in our laboratory (Winters et al., 1995). The HPLC system (Thermo Electron Corporation) consisted of a Finnigan Spectra System vacuum membrane degasser (model SCM1000), a gradient pump (model P2000), autosampler (model AS3000), and a fluorescence detector (model FL3000) with λex=330 nm and λem=376 nm. The HPLC column used was a Reliasil ODS-1 C18 column (5-μm packing material) with 250×4.6 mm i.d (Column Engineering, Ontario, CA). The mobile phase (70% acetonitrile and 30% water) was adjusted to a pH of 2 with acetic acid and o-phosphoric acid. The NPM derivatives of GSH were eluted from the column isocratically at a flow rate of 1 ml/min. The cell pellets obtained were homogenized in 1 ml of serine borate buffer (SBB,100 mM Tris buffer containing 10 mM borate and 5 mM serine with 1 mM diethylene triaminepentacetic acid; pH=7.4), centrifuged, and 250 μl of the supernatant were added to 750 μl of 1 mM NPM. The resulting solution was incubated at room temperature for 5 min, and the reaction was stopped by adding 10 μl of 2N HCl. The samples were then filtered through a 0.45 μm filter and injected into the HPLC system.

3.1.7. Determination of Malondialdehyde (MDA). The MDA levels were determined according to the method described elsewhere (Draper et al., 1993). Briefly, 550 µl of 5% trichloroacetic acid (TCA) and 100 µl of 500 ppm butylated hydroxytoluene (BHT) in methanol were added to 350 µl of the cell homogenates, and boiled for 30 min in a water bath. After cooling on ice, the mixtures were centrifuged, and the supernatant was collected and mixed 1:1 with saturated thiobarbituric acid (TBA). The mixture was again heated in a water bath for 30 min, followed by cooling on ice. 500 µl of the mixture were extracted with 1 ml of n-butanol and centrifuged to facilitate the separation of phases. The resulting organic layers were first filtered through 0.45 µm filters and then injected into the HPLC system (Shimadzu, US), which consisted of a pump (model LC-6A), a Rheodyne injection valve and a fluorescence detector (model RF 535). The column was a 100×4.6 mm i.d C18 column (3 µm packing material, Astec, Bellefonte, PA). The mobile phase used contained 69.4% sodium phosphate buffer, 30% acetonitrile, and 0.6% tetrahydrofuran. The fluorescent product was monitored at $\lambda ex= 515$ nm and $\lambda em= 550$ nm. Malondialdehyde bis (dimethyl acetal), which gives malondialdehyde on acid treatment, was used as a standard.

3.1.8. Mitochondrial Membrane Potential ($\Delta\Psi m$). Mitochondrial membrane potential was determined using potentiometric fluorescent dye JC-1 (5,5′,6,6′-tetrachloro-1,1′,3,3′-tetraethylbenzimidazolyl carbocyanine iodide; Invitrogen, San Diego, CA, USA). hCMEC/D3 cells were cultured in glass bottom petri dishes and were treated with AZT + IDV (50 µM, 100 µM , 200 µM) for 72 hr. The cells were washed twice with PBS and then incubated with JC-1 dye (1 µg/ 1 ml) in media for 30 min. The cells were then washed and placed under a fluorescent microscope in phenol red free

media. The stained cells were observed with an Olympus IX51 inverted microscope at
600× total magnification with a UPLFLN 60 X NA 1.25 objective. FITC (EX 482/35
506DM EM536/40) and TexasRed (EX 562/40 593DM EM 692/40) filters were used
(Brightline). Images were captured with a Hamamatsu ORCA285 CCD camera. The
shutters, filters and camera were controlled using SlideBook software (Intelligent
Imaging Innovations, Denver, CO).

3.1.9. Measurement of ATP Levels. Total ATP was quantified using a
commercially available luciferin–luciferase assay kit (ENLITEN ATP assay kit,
Promega, WI). A series of dilutions ranging from 0 to $1x10^{-13}$ M of the ATP stock
standard were made using ATP free water supplied in the kit. Using sterile disposable
tips, 100 µl aliquots of standards were pipetted into a clean 96-well microplate.
Additionally, 100 µl of cell lysate containing an equal amount of protein was placed into
the 96 well microplate. Once all of the standards and samples were pipetted, 100 µl
aliquots of luciferin–luciferase mixture from the ATP assay kit were dispensed into the
wells. Luminescence was measured after 15 min at 37°C using a luminometer (Fluostar,
BMG Labtechnologies, Durham, NC, USA). The mean value of the luminescence was
calculated for each treatment and plotted.

3.1.10. Catalase Activity. The activity of catalase (CAT; EC 1.11.1.6) was
measured spectrophotometrically at 240 nm, following the exponential disappearance of
hydrogen peroxide (H_2O_2; 10 mM), according to the method describe elsewhere (aebi,
1984). Cell pellets were homogenized in phosphate buffer (50 mM, pH 7.4) containing 1
mM EDTA and centrifuged at 8500 g for 10 min. An appropriate volume of supernatant

was mixed with phosphate buffer (50 mM, pH 7.0) and the reaction was initiated by

adding a H_2O_2 solution. The decrease in absorbance at 240 nm was measured for 2 min.

The catalase activity was calculated using $\Delta A240/min$ from the initial linear portion of

the curve and expressed as units/mg protein. One unit is defined as the amount of enzyme

that decomposes one micromole of H_2O_2 per minute under specified conditions of

temperature and pH (25 °C; pH 7.0).

3.1.11. Western Blot Analysis. Cell homogenates were prepared in a lysis buffer

(0.5% triton-x-100, 50 mM NaCl, 10 mM Tris, 1 mM EDTA, 1 mM EGTA, 2 mM

sodium vanadate, 0.2 mM PMSF, 1 mM HEPES, 1 μg/ml leupeptin, and 1 μg/ml

aprotinin). The cytosolic extracts were cleared by centrifugation at 12,000 x*g* for 15 min

at 4°C, and the protein concentration was estimated using a Bio-Rad 250 protein assay kit

(Bio-Rad, Hercules, CA). Protein samples (40 μg) were resolved by electrophoresis on a

12% sodium dodecyl sulfate (SDS) polyacrylamide gel (120v, 1.5 hr) in a running gel

buffer containing 25 mM Tris, pH 8.3, 162 mM glycine, and 0.1% SDS. The samples

were transferred to nylon membrane for 1 hr and 20 min at 350 mA. The membranes

were incubated overnight in a mixture of T-TBS with 0.1% Tween in 2% milk and the

respective antibodies caspase-3 (Santa Cruz biotechnology, Santa Cruz, CA), cytochrome

c , GAPDH (Cell Signaling Technology, Inc, Danvers, MA) and manganese superoxide

dismutase (MnSOD; Cayman Chemicals, Ann Arbor, MI) in 1:1000 dilution.

Subsequently, the membrane was incubated in the respective secondary antibody

(1:10,000) for 1 hr at room temperature. Final visualization was carried out with the

enhanced chemiluminescence kit (Bio-Rad, Hercules, CA). The protein bands were

quantified by densitometry (Haorah et al., 2005).

3.1.12. Apoptosis Measurement. Apoptosis was quantified using the ethidium bromide and Acridine Orange assay (Duke and cohen, 1999). Briefly, control and treated cells (10^6) were transferred to microcentrifuge tubes and pelleted for 10 min at 1,000 xg. After centrifugation, the cell-rich pellets were resuspended in a mixture containing 2 μl of ethidium bromide (100 μg/ml) and 2 μl of Acridine Orange (100 μg/ml). The stained cells were observed with an Olympus IX51 inverted microscope at 600× total magnification with a UPLFLN 60 X NA 1.25 objective. FITC (EX 482/35 506DM EM536/40) and TexasRed (EX 562/40 593DM EM 692/40) filters were used (Brightline). Images were captured with a Hamamatsu ORCA285 CCD camera. The shutters, filters and camera were controlled using SlideBook software (Intelligent Imaging Innovations, Denver, CO). Live, apoptotic, and necrotic cells were differentiated from each other using fluorescence microscopy on the basis of definitive nuclear and cytosolic fluorescence and distinct morphological changes, including membrane blebbing, nuclear and cytosolic condensation, and nuclear fragmentation.

3.1.13. Measurement of Intracellular Calcium Concentration ($[Ca^{2+}]_{in}$). hCMEC/D3 cells were briefly plated on glass-bottom dishes and allowed to attach for 24 hr. The cells were exposed to different concentrations of AZT + IDV combination for 72 hr. The cells were washed with PBS and were incubated for 20 min to allow efficient loading of membrane permeable Fura-2 AM in a serum-free media. The entire medium was then removed and the cells were washed with PBS twice to eliminate extracellular Fura-2AM. Following this wash, serum-free medium was added to the cells, which were then allowed to reach homeostasis by incubation for the remaining 20 min at 37 ^{0}C. The cells were then placed on the stage of an inverted fluorescence microscope

(*InCyt Basic IM* Fluorescence Imaging System, Intracellular Imaging Inc.). The cells were excited at 340 nm and 380 nm while emission was monitored at 510 nm at an acquisition rate of 10 Hz. The ratio of fluorescence measured after excitation at the two wavelengths (F_{340}/F_{380}) was proportional to the free calcium concentration. In each independent experiment, 25 cells were selected to measure the $[Ca^{2+}]_{in}$ and averaged (Huang et al., 2010).

3.1.14. Trans-Endothelial Electric Resistance (TEER) Measurement.

Transendothelial electric resistance (TEER) measurement by an EVOM voltohmmeter (World Precision Instrument, Sarasota, FL, USA) assessed the tightness of the hCMEC/D3 monolayer. hCMEC/D3 cells were seeded onto collagen-coated inserts with a pore size of 0.4 μm at densities of 15×10^3/well, and allowed to culture until a monolayer formed (4–7 days). The cell monolayer was then treated with AZT + IDV or a serum-free media for 72 hr. After this, the media was replaced with 150 μl of fresh medium. The insert containing the cell monolayer was then transferred in to a fresh plate containing 500 μl of serum-free medium. The TEER reading was recorded immediately. TEER values were calculated as: Resistance$\times$0.33 Ωcm^2 (insert surface area) and were expressed as a percentage of control. Thus, resistance is inversely proportional to the effective membrane (Zhang et al., 2009).

3.1.15. Dextran Permeability Study.

hCMEC/D3 cells were seeded onto collagen-coated inserts with a pore size of 0.4 μm at densities of 15×10^3/well, and allowed to culture until a monolayer formed. The cell monolayer was then treated with AZT or serum-free media for 72 hr. After this, the medium in the insert was replaced

with 150 µl of FITC labeled dextran, and was transferred to a fresh plate well, containing
500 µl of serum-free medium. The plates were incubated for 30 min at room temperature,
and 100 µl of the plate's well solution were removed and transferred to a 96-well plate.
Fluorescence was read with a 485 nm excitation and 530 nm emission, using a microplate
reader (Fluostar, BMG Labtechnologies, Durham, NC, USA) (Zhang et al., 2009).

3.1.16. Determination of Protein. Protein levels of the cell samples were
measured by the Bradford method (Bradford, 1976). Concentrated Coomassie Blue (Bio-
Rad, Hercules, CA) was diluted 1:5 (v/v) with distilled water. 20 µl of the diluted cell
homogenate were then added to 1.5 ml of this diluted dye, and absorbance was measured
at 595 nm using a UV spectrophotometer (Shimadzu Scientific Instruments, Columbia,
MD). Bovine serum albumin (BSA) was used as the protein standard.

3.1.17. Statistical Analysis. Group comparisons were performed using the one-
way analysis of variance (ANOVA) test and the TUKEYS post hoc test. Statistical
analyses were made using GraphPad Prism 5.01 (GraphPad Software Inc., La Jolla, CA).
Statistical significance was set at $p < 0.05$.

4. *IN VITRO* RESULTS

4.1. VIABILITY AND OXIDATIVE STRESS STUDIES

4.1.1. Antiretroviral Drugs Decrease Viability. To determine whether the HAART drug combination affects the viability of endothelial cells, we treated hCMEC/D3 cells with AZT + IDV. Effects of AZT + IDV on cell viability of hCMEC/D3 were determined by using the calcein AM assay. Cells were treated with drug combinations ranging from 5 µM to 200 µM each, used in previously reported studies with immortalized endothelial cells (Collier et al., 2003). Treatment with drugs for 24 hr did not show a significant trend by ANOVA, except for the 50 µM, 100 µM, and 200 µM treated groups ($p<0.05$). However, analysis of individual differences with Tukey's post test showed that only the highest concentration (200µM) was different from that of the 50µM and 100 µM treated groups ($p<0.05$), and produced a moderate decrease in cell viability (~ 21% decrease) (Figure 4.1). Treatment with AZT + IDV induced a more prominent decrease in viability after 72 hr (Figure 4.2), in a dose-dependent manner. 50 µM, 100 µM, and 200 µM concentrations of AZT + IDV caused an increase in cell death (approximately 21%, 43%, and 65%, respectively, at $p<0.05$), and, hence, these concentrations of AZT + IDV were used for further studies.

The cytotoxic effect of AZT+ IDV treatment assessed using light microscopy shows the deleterious effects on viability. Figure 4.3 shows the effect of AZT+IDV on morphology of hCMEC/d3 cells. Control cells appear to be well-differentiated whereas treated group with AZT+IDV shows round and floating cells indicating cells undergoing death. Cells treated with 100 µM of AZT or IDV alone showed that AZT was more toxic than IDV in these cells ($p<0.05$). IDV and AZT alone treated cells showed a decrease in

viability of 23% and 34%, respectively, whereas cells treated with an AZT + IDV

combination showed only a 43% decrease in viability (Figure 4.4).

4.1.2. Effect of HAART Drugs on ROS Production. To examine the role of

oxidative stress in endothelial cell death, we measured the levels of ROS in endothelial

cells treated with drugs using the $DCFH_2$-DA fluorescent assay. ROS are a highly

transient species and in order to measure them, an intermediate time point of 48 hr was

selected. Endothelial cells were incubated with AZT + IDV for 48 hr followed by

washing to remove the drugs. Re-incubation of hCMEC/D3 cells in the presence of the

dye DCF for 0.5 hr resulted in an increase in fluorescence compared to control.

Treatment with AZT + IDV induced a 1.5 to 2 fold increase in ROS production after the

48-hr treatment (Figure 4.5). Although the ROS levels were different than those of the

control ($p<0.05$), no significant difference was observed between those of treated groups.

4.1.3. Effect of HAART Drugs on GSH levels. Oxidative stress or a high level

of ROS generation leads to the decline in cellular antioxidants like GSH. The levels of

GSH were measured after treatment with AZT+IDV to further assess the role of oxidative

stress in cytotoxicity. The levels of glutathione in all treated groups were significantly

lower than that of the control (Figure 4.6). In the AZT + IDV treated groups, dose-

dependent decreases in the GSH levels were observed. Cells treated with 200 μM

AZT+IDV had a 65% decrease in GSH levels, as compared to controls, whereas those

treated with 100 μM and 50 μM doses experienced decreases of 50 % and 40% with

respect to that of the control ($p<0.05$).

4.1.4. HAART Effects on Lipid Peroxidation Levels. An increase in ROS and a decrease in GSH led to high levels of reactions between free radicals and membrane lipids, causing lipid peroxidation in the cells. This was estimated by measuring the levels of malondialdehyde (MDA), a stable by-product of lipid peroxidation. MDA levels were significantly increased in all treated groups, as compared to control. MDA levels in the group treated with 50 µM (Figure 4.7) were arithmetically higher, but this did not reach statistical significance. A 1.5- to 3-fold increases in MDA levels were observed in the cells treated with 100 µM and 200 µM doses of AZT+IDV, as compared to the controls ($p < 0.05$).

4.1.5. Antioxidant Enzyme Activity. Catalase is a common enzyme found in nearly all living organisms that are exposed to oxygen, where it functions to catalyze the decomposition of hydrogen peroxide to water and oxygen. Activity of catalase in AZT+ IDV treated hCMEC/D3 cells is shown in figure 4.8. Catalase activity decreased significantly in cells treated with AZT+IDV treated groups ($p<0.05$). A dose dependent decrease in catalase activity was observed indicating that AZT+IDV treatment modified the ability of the cells to cleave hydrogen peroxide and protect cells.

4.2. HAART DRUGS DISRUPT MITOCHONDRIAL FUNCTION

4.2.1. Dissipation of Mitochondrial Membrane Potential (ΔΨm). One important intracellular target of drugs is mitochondria, which is also a source of ROS inside cells. Any disruption in mitochondrial permeability and function can be assessed by measuring the changes in mitochondrial membrane potential (ΔΨm). The decrease in ΔΨm was demonstrated by using membrane permeable potentiometric dye, JC-1. Cells

with mitochondrial dysfunction showed primarily green fluorescence, whereas healthy

cells were differentiated with red and green fluorescence. As shown in Figure 4.9, control

cells stained both red and green, whereas a dose-dependent decrease in red fluorescence

was seen in treated groups. Although the 200 µM treated group showed specks of red

fluorescence, these images did not merge into the cytoplasmic area of cells (green

fluorescence), as seen in previous groups, and appeared to be floating dye aggregates.

Decreases in the red fluorescence across treated groups indicated that AZT + IDV

treatment dissipated $\Delta\Psi m$ in the BBB cells. These results support our hypothesis that

AZT + IDV treatment depolarizes the mitochondria membrane potential, disrupting the

mitochondrial function, and resulting in cell death.

4.2.2. Changes in ATP levels. ATP levels were measured as another test for

mitochondrial function. Treatment with AZT + IDV after 72 hr resulted in a dose-

dependent decrease in ATP levels (Figure 4.10). Compared to control, the ATP levels

decreased 20-50 % in treated groups ($p<0.05$). These results also add to the evidence that

HAART drugs affect mitochondrial function.

4.2.3. Effect of AZT+IDV on MnSOD Protein Expression. hCMEC/D3 cells

were maintained in supplemented EGM-2 (see Methods). Cells were incubated with 50

µM, 100 µM, and 200 µM of AZT + IDV for 72 hr. MnSOD protein expression was

monitored by western blot analysis. The levels of protein expression of MnSOD appeared

to be slightly elevated in the 50 µM treated group, whereas no change was detected in the

100 µM sample. There was, however there was a significant decrease in the expression of

MnSOD protein in the 200 µM treated group (Figure 4.11).

4.3. EFFECT OF HAART DRUGS ON APOPTOTIC CELL DEATH

4.3.1. Effect of HAART on Cytochrome *c* and Procaspase-3 Expression. The disruption of mitochondrial membrane function is known to result in the release of the mitochondrial enzyme cytochrome *c* into the cytosol. The levels of cytochrome *c* release were measured to determine if changes in mitochondrial membrane potential correlate with the initiation of apoptosis (Skulachev, 1998). Figure 4.12 shows levels of cytochrome *c* released from mitochondria into the cytoplasm. There was an increase (~1.5 -2.0 fold) in cytochrome c released in 50 µM and 100 µM ($p<0.05$). Cytochrome *c* levels in 200 µM treated group were arithmetically higher, but were not significant when compared to that of the control. As additional evidence of apoptosis occurring in endothelial cells treated with AZT + IDV, we measured the levels of procaspase-3 protein, as shown in Figure 4.13. Although there was an increase in the expression of procaspase-3 in all treatments, there was an even higher increase in the 50 µM - treated cells, as compared to other treated groups.

4.3.2. Apoptosis Detection Using Acridine Orange and Ethidium Bromide. To corroborate that apoptosis had been induced by AZT+IDV, hCMEC/D3 cells were analyzed in the presence of acridine orange and ethidium bromide staining (AO/EB staining). Acridine orange is a vital dye that will stain both live and dead cells, whereas ethidium bromide will stain only those cells that have lost their membrane integrity (Kasibhatla et al., 2006). As a control, cells were cultured in a complete media and stained with AO/EB (Figure 4.14A). Cells stained green represented viable cells, whereas yellow staining represented early apoptotic cells, and reddish or orange staining indicated

late apoptotic cells. As shown in Figure 4.14B, 50 µM treated hCMEC/D3 cells showed

changes in cellular morphology, including chromatin condensation, membrane blebbing,

and fragmented nuclei. Figs. 4.14C and 4.14D showed similar features for 50 µM

treated cells (Figure 4.14B), but had extra features of late stage apoptotic bodies when

hCMEC/D3 cells were treated with 100 µM and 200 µM of the AZT + IDV treated

group.

4.4. INTRACELLULAR CALCIUM [CA^{2+}]$_{in}$ MEDIATES APOPTOSIS

It is now known that intrinsic pathways in apoptosis involve the exchange of

Ca^{2+} signals between the ER and the mitochondria that coordinate the precommitment

phase of apoptosis (Pinto et al., 2008). It has also been shown that oxidative stress

increases the intracellular calcium concentration leading to activation of endonucleases,

which degrade DNA and, ultimately, contribute to cell death (Annuziato et al., 2003) In

order to explore the role of calcium in apoptosis by AZT + IDV, we assessed the levels of

[Ca^{2+}]$_{in}$ using fluorescent microscopy. We detected a 1.5-2.5 fold increase ($p<0.05$) in

calcium levels in the 100 µM and 200 µM treated groups, when compared to levels in the

control (Figure 4.15). Although the 50 µM treated group showed an increase in

[Ca^{2+}]$_{in}$ levels, these were not statistically different than those of the control, but 100 µM

and 200 µM treated groups were different from 50 µM treated group ($p<0.05$). These

results imply that [Ca^{2+}]$_{in}$ mediates the mitochondrial permeability transition, thereby

releasing intra-mitochondrial contents like cytochrome *c* during apoptosis.

4.5. EFFECT OF HAART DRUGS ON THE BBB INTEGRITY

Regulation of the flow of substances through intercellular spaces depends on the integrity of the BBB. Permeability studies, such as dextran cell permeability assay and TEER assays were used in this study to assess the integrity of a monolayer of endothelial cells as they simulate the integrity of the BBB (Gandhi et al., 2010). The resistance measured across the monolayer of cells showed a decrease in resistance of approximately 10-30% across the treated groups (Figure 4.16A). To further support these findings, we also measured the amount of FITC labeled dextran that leaked across the monolayer using fluorometry after treatment. In agreement with the data for TEER, there was a 10-60% increase in the permeability of the layer, as seen by the increase in fluorescence across the treated groups. In both of these studies, the 100 µM and 200 µM treated groups were different from the control ($p<0.05$). Although the 50 µM treated group was not significant when compared to control, they were arithmetically higher than control. Tukey post hoc analysis showed that the 100 µM and 200 µM treated groups was different from the 50 µM treated group ($p<0.05$).This indicated that intercellular junctions between the endothelial cells were compromised with HAART treatment (Figure 4.16B).

4.6. EFFECT OF NACA ON AZT+IDV INDUCED TOXICITY

4.6.1. Cytotoxicity Studies. Figure 4.17 displays the results of cytotoxicity studies of NACA in hCMEC/D3 cells. Cells were incubated with 0.25, 0.5, 0.75, 1, 2, 5, 10 mM NACA for 24 h, after which calcein AM was added and fluorescence levels were measured. Reagent controls and cell controls were included. These results indicated that

except the 10 mM NACA treated group all the other groups had cell viability comparable

to that of the control. The highest concentration of 10 mM NACA appeared to be mild

cytotoxic to cells, so a minimal dose of 2 mM NACA, the dose without any cytotoxic

effects was selected for our studies.

The protective effect of NACA in AZT+IDV induced cell death in hCMEC/D3

cells is shown in Figure 4.18. Although the cells appeared to be rescued from the

cytotoxic effect of AZT+IDV drugs, the increase in cell viability appear to be arithmetic,

rather than significant, when compared to the treated group. The viability in the

AZT+IDV treated group decreased to approximately 65%, when compared to control.

Pretreatment with NACA could only raise the viability to 77% when compared to control.

4.6.2. Reactive Oxygen Species (ROS) Levels. Our studies with AZT+IDV

showed a dose dependent increase in ROS levels in endothelial cells. In order to test the

effect of NACA on ROS production in AZT+IDV treated groups, cells were

preincubated with 2 mM NACA for 1 hr. Figure 4.19 shows the scavenging effect of

NACA on free radicals in treated cells. NACA pretreated hCMEC/D3 cells had

significantly lower levels of ROS when compared to that of the treated group ($p<0.05$)

and it appeared to be almost equal to that of the control. These results suggest that the

protective effect of NACA may partly be from the ability to scavenge free radicals in

oxidative stress.

4.6.3. NACA Effect on Glutathione (GSH) Levels. Depletion of cellular

antioxidants like GSH is commonly observed in oxidatively challenged conditions. Thiol

antioxidants are known to replenish cells with GSH levels in these situations, so we

tested the ability of NACA to increase GSH levels in AZT+IDV treated. Figure 4.20

shows the effect of NACA on GSH levels in drug treated groups. GSH levels in

endothelial cells in the NACA pretreated group had significantly high levels of GSH

(approximately ~70% of the control) when compared to that of the AZT+IDV treated

groups ($p<0.05$). These results suggest that NACA can prevent oxidative stress in cells by

being uses as substitute to GSH for scavenging free radicals or indirectly by increasing

the GSH levels.
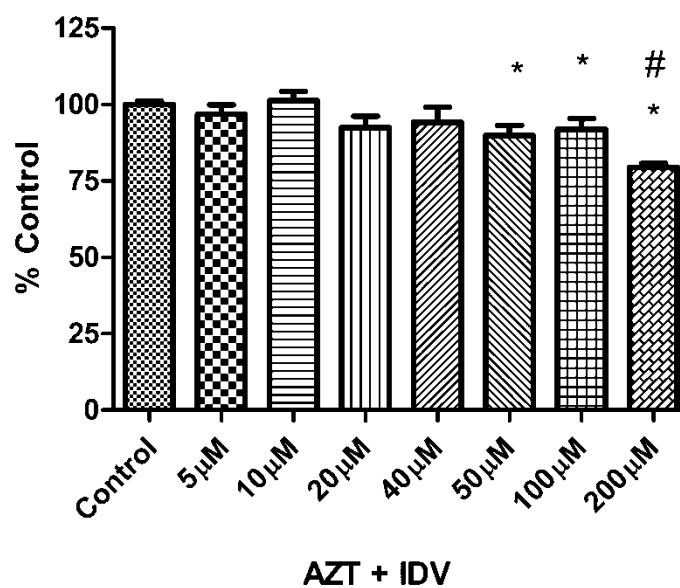
Figure 4.1. Effect of AZT + IDV treatment for 24 hr on viability. Effect of AZT + IDV treatment for 24 hr (5 µM-200 µM) on hCMEC/D3 cell viability as indicated by uptake of calcein. Results as mean percent of controls (Mean±SEM; n=5). * Statistical differences (p<0.05) as compared to untreated control. # Statistical difference (p<0.05) compared to 50 µM and 100 µM group.
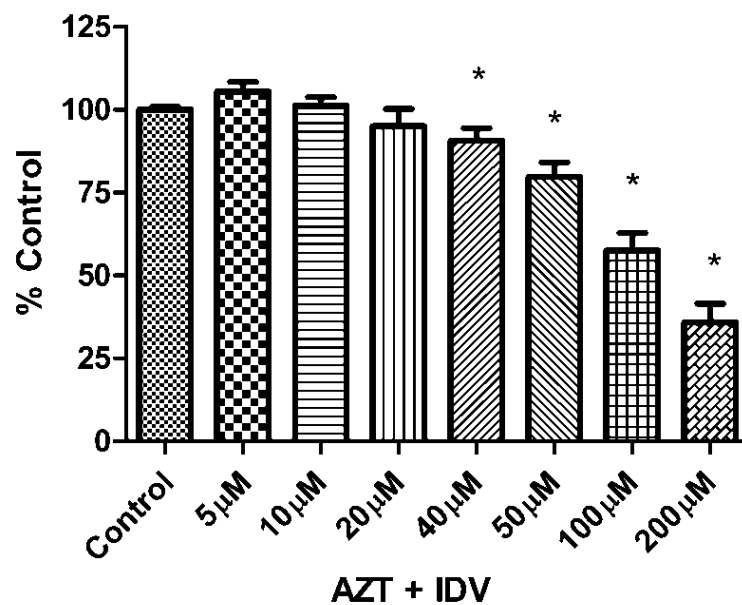
Figure 4.2. Effect of AZT + IDV treatment for 72 hr on viability. Effect of AZT + IDV treatment for 72 hr (5 µM-200 µM) on hCMEC/D3 cell viability, as indicated by uptake of calcein. Results as mean percent of controls (Mean±SEM; n=5). * Statistical differences (p<0.05) as compared to untreated control.
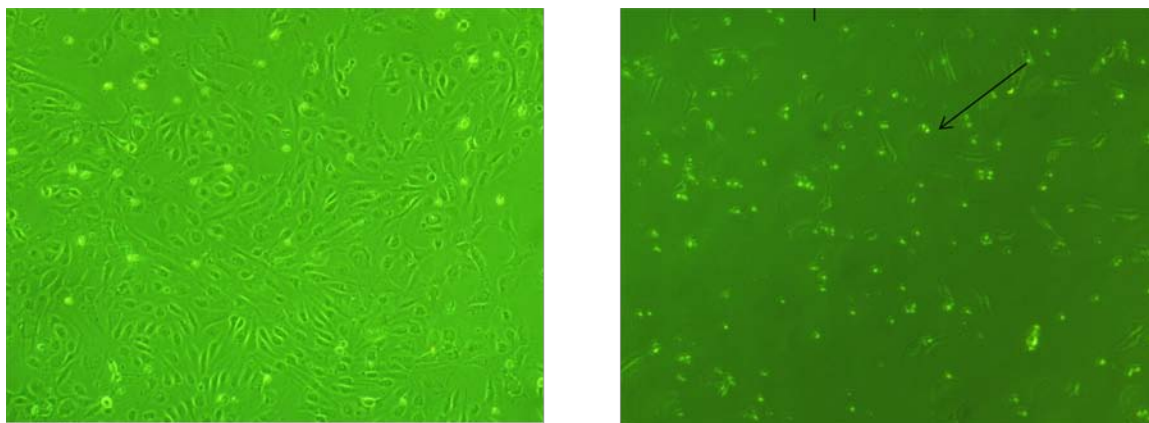
(A) Control   (B)   AZT+IDV (200 µM)

Figure 4.3. Morphological assessment of AZT +IDV treatment. hCMEC/D3 cells were treated with or without AZT+IDV (200 µM) for 72 hr. The morphology was assessed using an Olympus inverted microscope. Arrow indicates dead cells in 200 µM group.
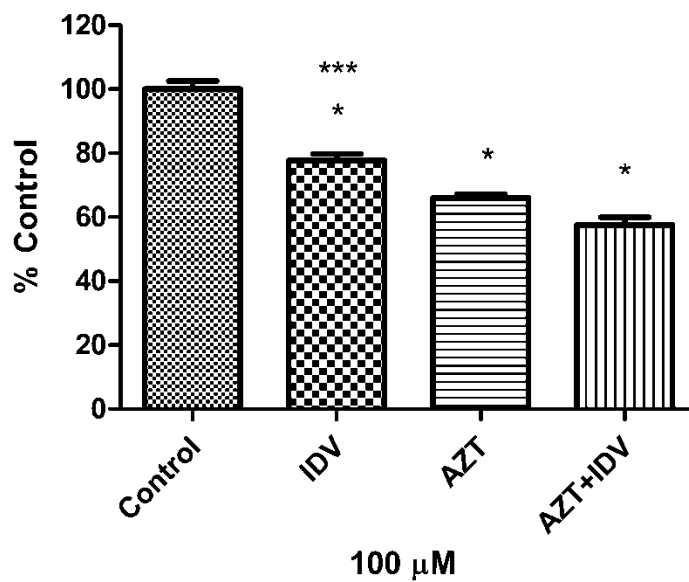
Figure 4.4. Effect of AZT or IDV alone on viability. Effect of AZT or IDV alone and in combination treatment (100 µM) for 72hr on hCMEC/D3 cell viability as indicated by uptake of calcein. Results as mean percent of controls (Mean±SEM; n=5). * Statistical differences (p<0.05) as compared to untreated control. *** Statistical difference (p<0.05) compared to AZT treated group.
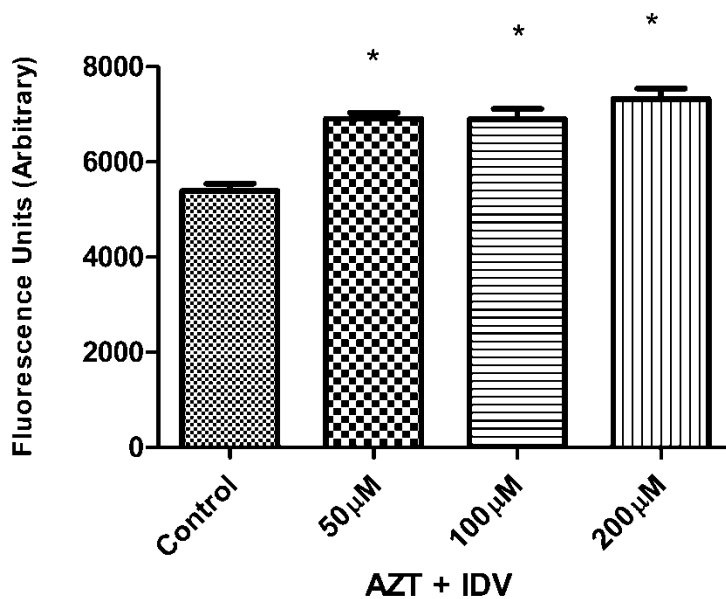
Figure 4.5. Reactive oxygen species (ROS) production. Reactive oxygen species (ROS) production induced in hCMEC/D3 cells treated with 50 µM, 100 µM and 200 µM, AZT +IDV for 48 hr. Cellular ROS levels were assessed using DCFH$_2$-DA. Results expressed as mean values (Mean±SEM; n=5). * Statistical differences (p<0.05) as compared to untreated control.
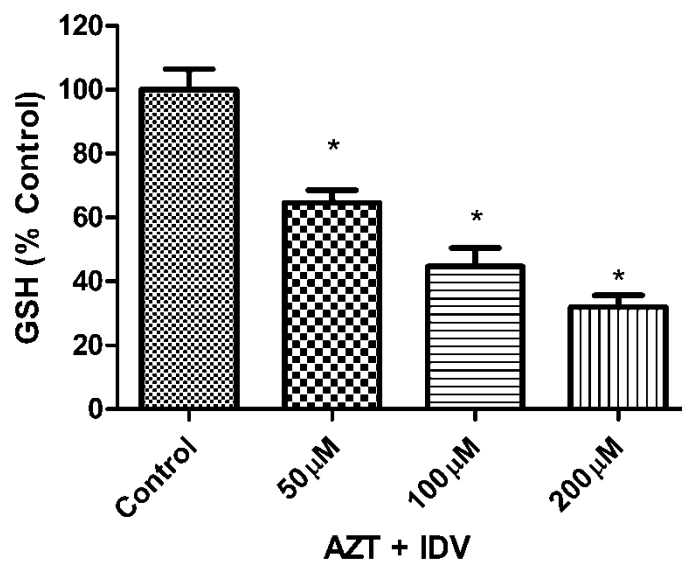
Figure 4.6. Glutathione (GSH). AZT + IDV (50 µM, 100 µM, and 200 µM) exposure led to intracellular glutathione (GSH) decrease in a dose-dependent manner. hCMEC/D3 cells were treated for 72 hr and GSH levels were measured using HPLC method described in Materials and Methods section. Results expressed as mean percent of controls (Mean±SEM; n=4). * Statistical differences (p<0.05) as compared to untreated control.
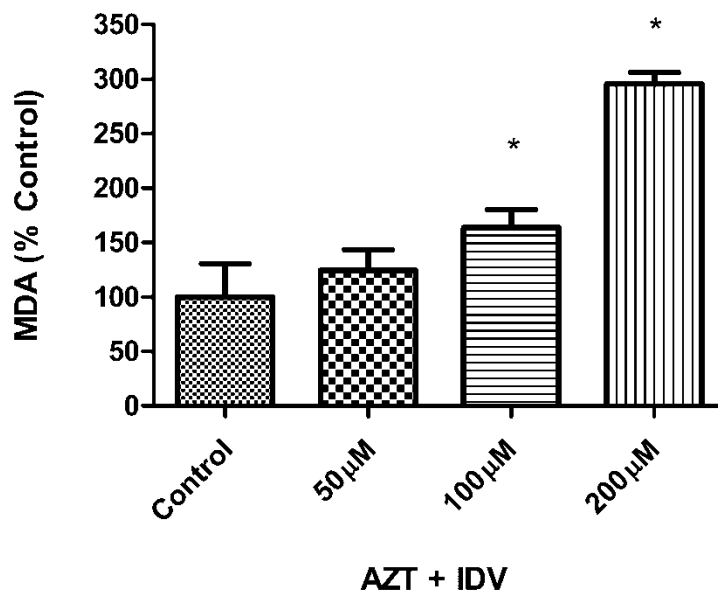
**Figure 4.7.** Lipid peroxidation levels. Lipid peroxidation in hCMEC/D3 cells. AZT + IDV (50 µM, 100 µM, 200 µM) treatment for 72 hr caused oxidative stress resulting in an increase in malondialdehyde (MDA) levels, a lipid peroxidation metabolite. MDA levels were measured using HPLC method described in the Materials and Methods section. Results expressed as mean percent of controls (Mean±SEM; n=4).). * Statistical differences (p<0.05) as compared to untreated control.
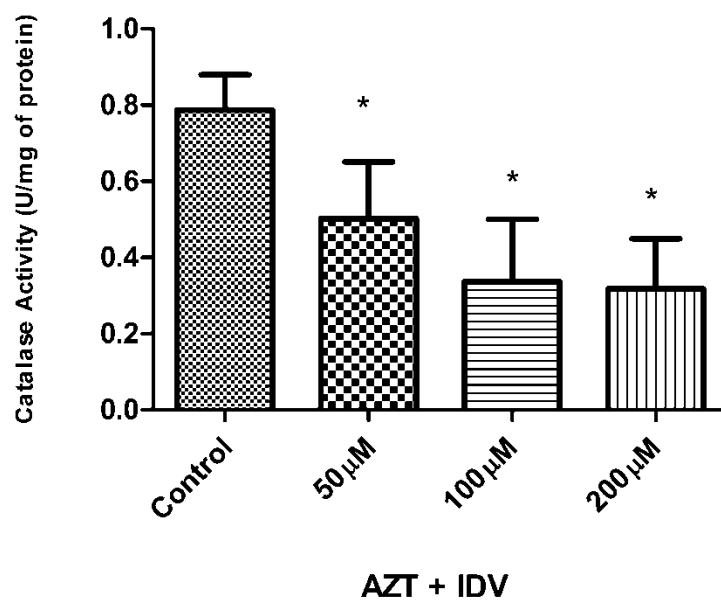
Figure 4.8. Effect of AZT+ IDV on antioxidant enzyme catalase activity. Cells were treated for 72 hr with the drug combination and activity was estimated using spectro photometric method. Each value is an average of at least triplicate values with standard error mean bars (n=4). * Statistical differences (p<0.05) as compared to untreated control.
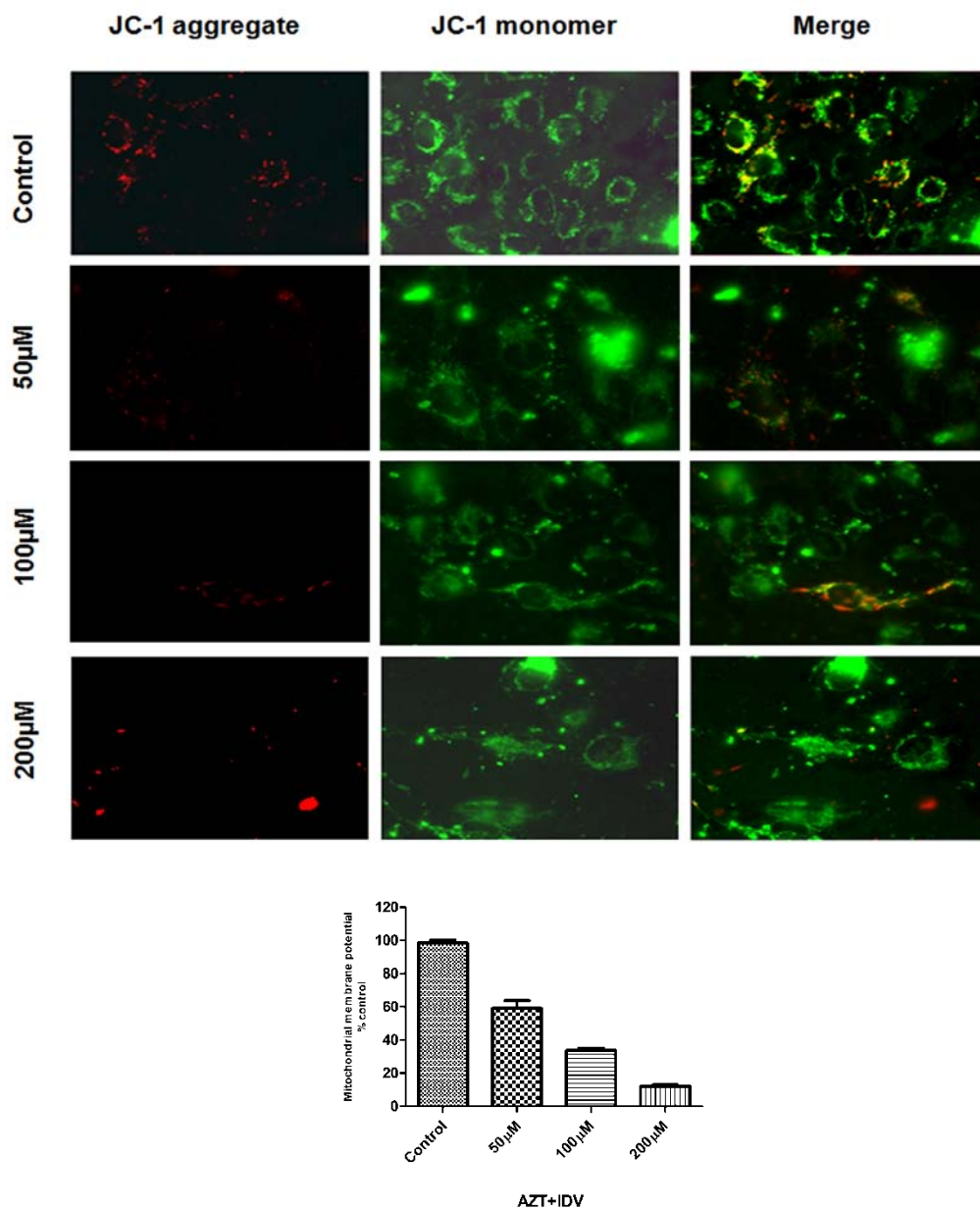
Figure 4.9. Analysis of mitochondrial membrane potential. ΔΨm was analyzed in adherent hCMEC/D3 after 72 hr of AZT+IDV treatment, using the potential-dependent aggregate-forming lipophilic cation JC-1 (5,5',6,6'-tetrachloro-1,1',3,3'-tetraethylbenzimidazole carbocyanide iodide). Left image represents JC-1 dye aggregation in mitochondria with intact membrane potential. Mitochondria exhibit red fluorescence if ΔΨm is preserved. Middle image represents JC-1 monomers exhibiting green fluorescence in cytoplasm of cells. Mitochondria in treated cells showed a dose-dependent decrease in red fluorescence due to loss of ΔΨm. Merged images are represented on extreme right. Each experiment was performed in triplicate (n = 3) and generated similar changes in fluorescence.
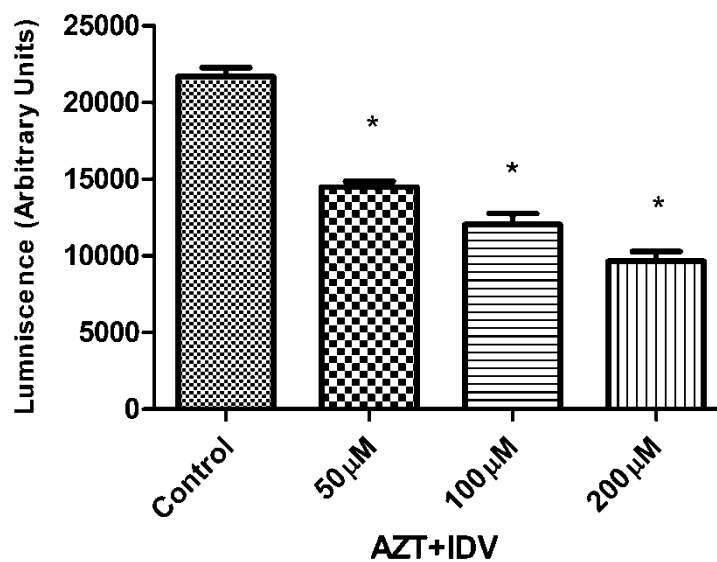
Figure 4.10. ATP levels. ATP levels were measured with the bioluminescence assay (Promega) in AZT + IDV (50 µM, 100 µM, 200 µM) treated cells for 72 hr. Exposure to drugs showed a dose-dependent decrease in ATP levels. * Statistical differences (p<0.05) as compared to untreated control (Mean±SEM; n=4).
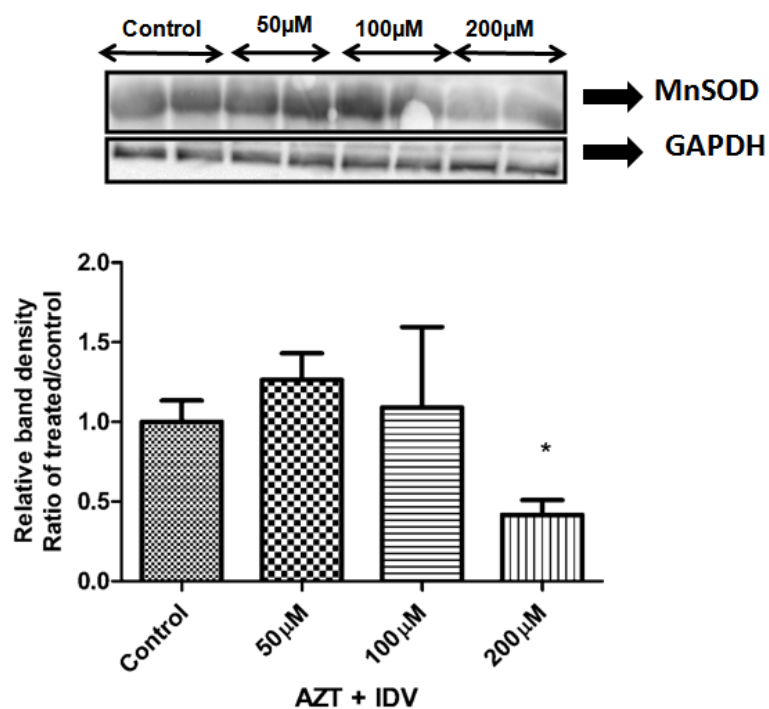
Figure 4.11. Expression of manganese superoxide dismutase protein. (MnSOD)The expression of manganese superoxide dismuatase in hCMEC/D3 cells treated with AZT + IDV for 72 hr Equal amounts of cellular protein were separated on 12% SDS-PAGE gels and transferred to nitrocellulose membranes as described in Materials and Methods. GAPDH was used as an internal control.
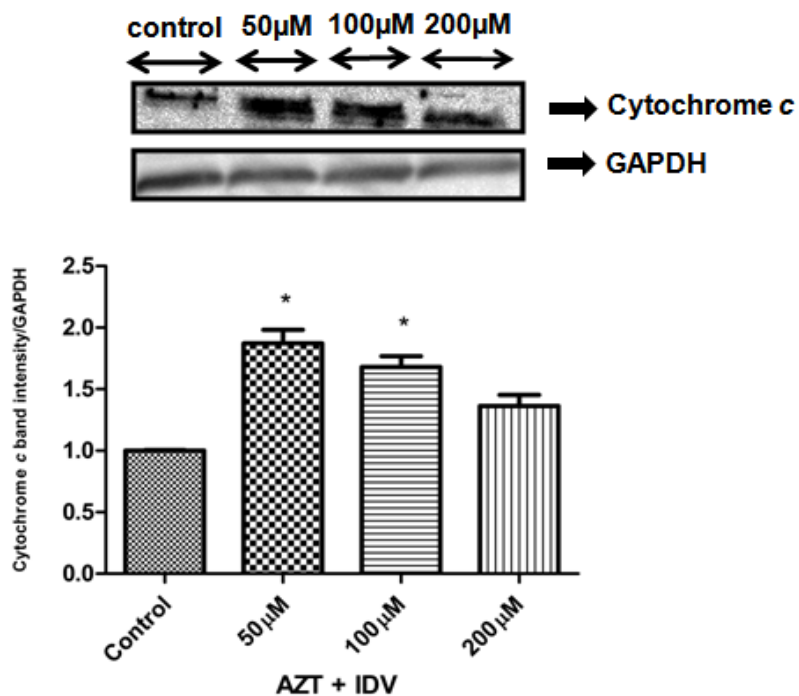
Figure 4.12. The expression of apoptosis-related protein cytochrome *c*. hCMEC/D3 cells treated with AZT + IDV for 72 hr. Equal amounts of cellular protein were fractionated on 12% SDS-PAGE gels and transferred to nitrocellulose membranes as described in Materials and Methods. GAPDH was used as an internal control.
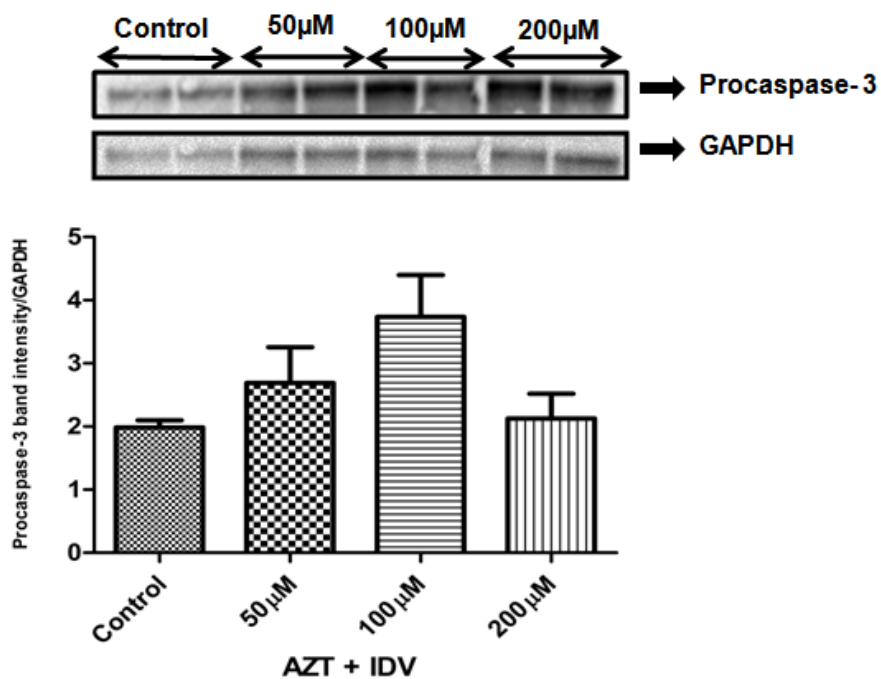
Figure 4.13. The expression of apoptosis-related protein procaspase-3. hCMEC/D3cells treated with AZT + IDV for 72 hr. Equal amounts of cellular protein were separated on 12% SDS-PAGE gels and transferred to nitrocellulose membranes as described in Materials and Methods. GAPDH was used as an internal control.
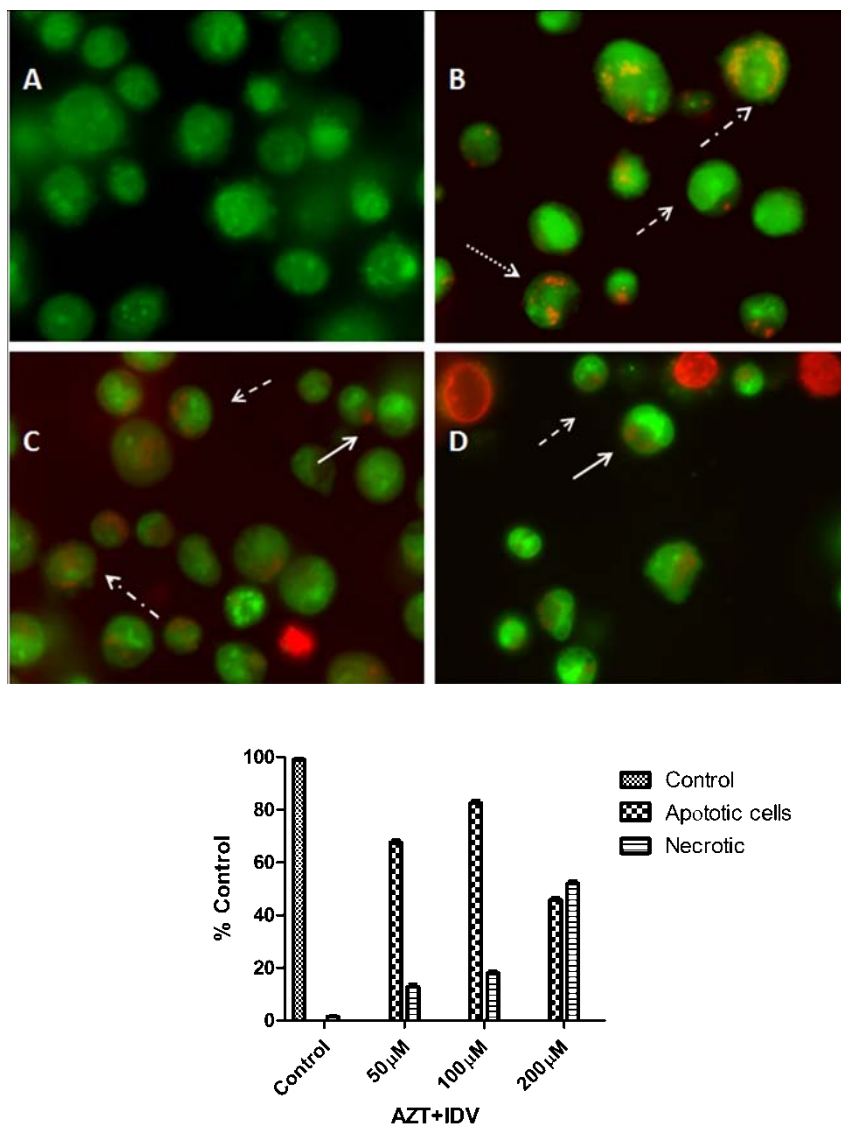
Figure 4.14. Apoptosis detection using acridine orange with ethidium staining. hCMEC/D3 cells were treated with AZT + IDV for 72 hr and were stained with AO/EB mixture. (A) Control and viable cells appearing only green due to acridine orange staining. (B) 50 µM treated hCMEC/D3 cells showing changes in cellular morphology for early apoptosis and appearing orange with ethidium staining. Dashed arrow indicates cells with chromatin condensation; rounded dotted arrow indicates cells with fragmented nuclei; dashed dotted arrow indicates cells with membrane blebbing. (C) 100 µM treated group showing morphological similar to 50 µM treated group with some late apoptotic features. Full white arrow indicates the presence of apoptotic bodies. (D) 200 µM treated group with cells showing chromatin condensation and late apoptotic features like apoptotic bodies. Necrotic cells appearing red with ethidium staining. Each experiment was performed in triplicate (n = 3) and generated similar morphological features.
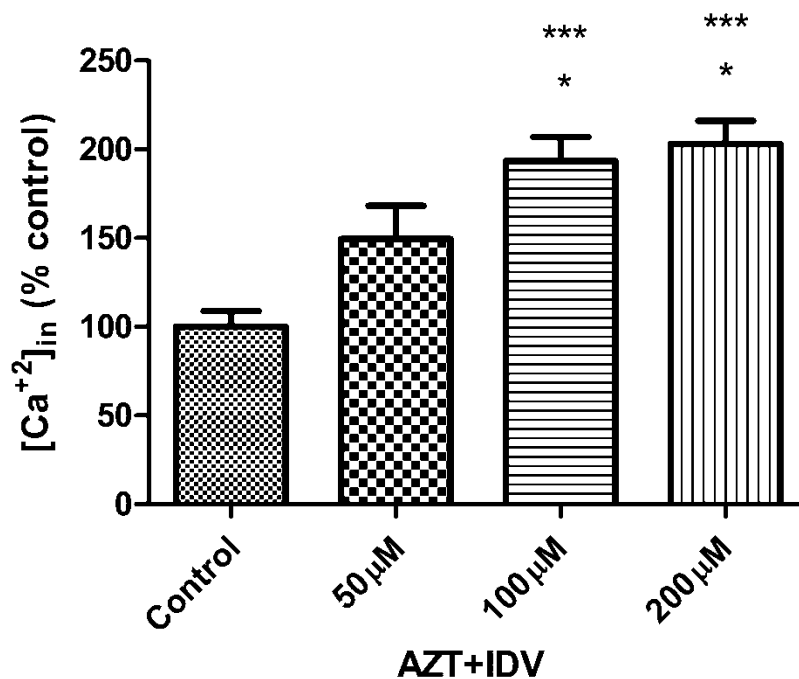
Figure 4.15. Effect of AZT + IDV treatment on intracellular calcium levels [Ca^{2+}]$_{in}$
  hCMEC/D3 cells were treated with AZT + IDV for 72 hr and calcium levels were
measured as described in Material and Methods section. Results expressed as mean
percent of controls (Mean±SEM; n=3). Each value is average of atleast triplicate values
with standard error mean bars. * Statistical differences (p<0.05) as compared to untreated
control. *** Statistical difference (p<0.05) compared to 50 µM treated group.
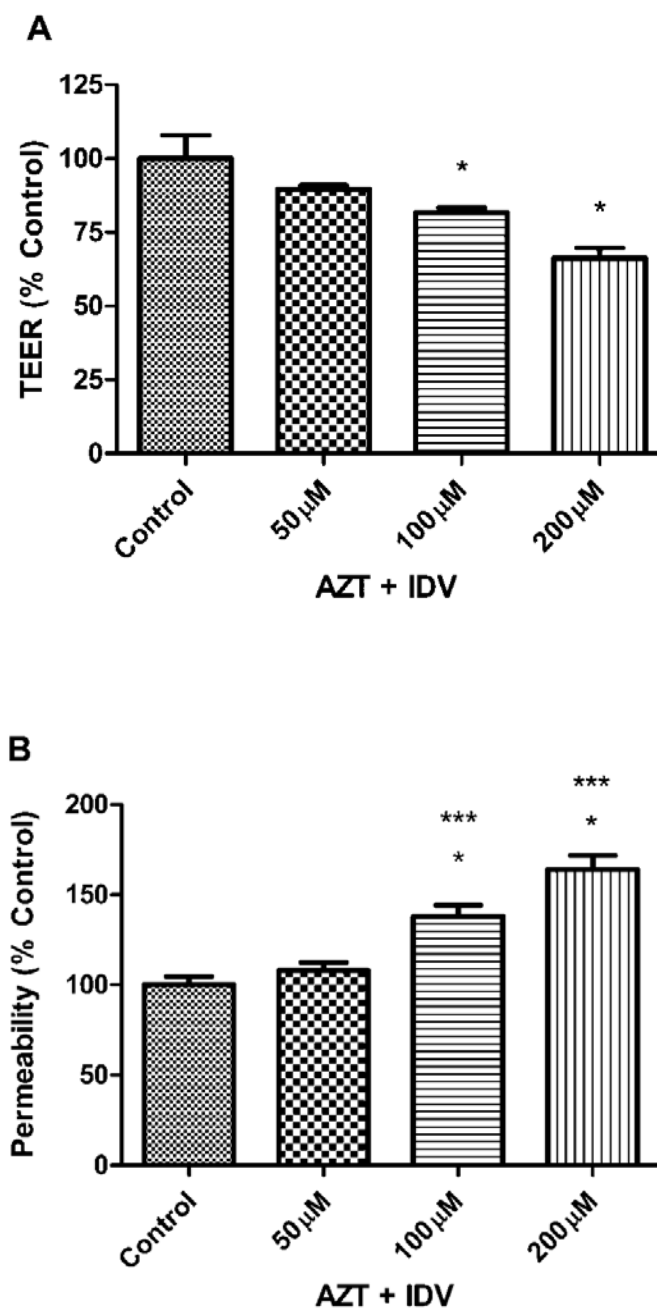
Figure 4.16. Effect of AZT + IDV on TEER and dextran permeability. (A) AZT + IDV treatment significantly reduced TEER, and TEER measurement across the hCMEC/D3 monlayer measured the BBB integrity and tightness. TEER values recorded in ohms (Ω)/insert area were corrected to Ω/cm^2 from three experiments in triplicate. Results as mean percent of control (Mean±SEM; n=3). (B) Monolayer treatment for 72 hr with AZT + IDV increased the permeability of FITC-labeled dextran across the BBB. Fluorescence measured was then expressed as mean percent of control (Mean±SEM; n=3). * Statistical differences (p<0.05) as compared to untreated control. *** Statistical difference (p<0.05) compared to 50 µM treated group.
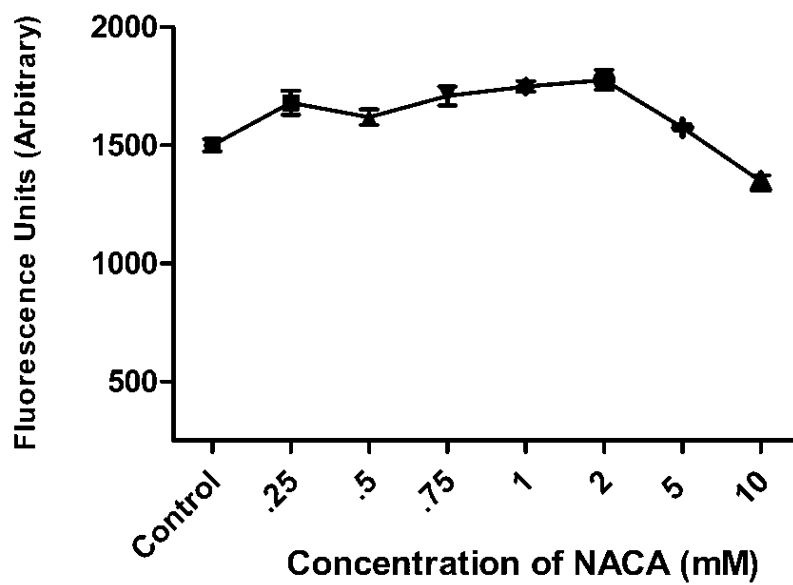
Figure 4.17. Effect of NACA on hCMEC/D3 cell viability. Cells were treated with different concentrations of NACA in serum free media and viability was assessed using calcein assay. Each value is an average of at least triplicate values with standard error mean bars (Mean±SEM; n=5).
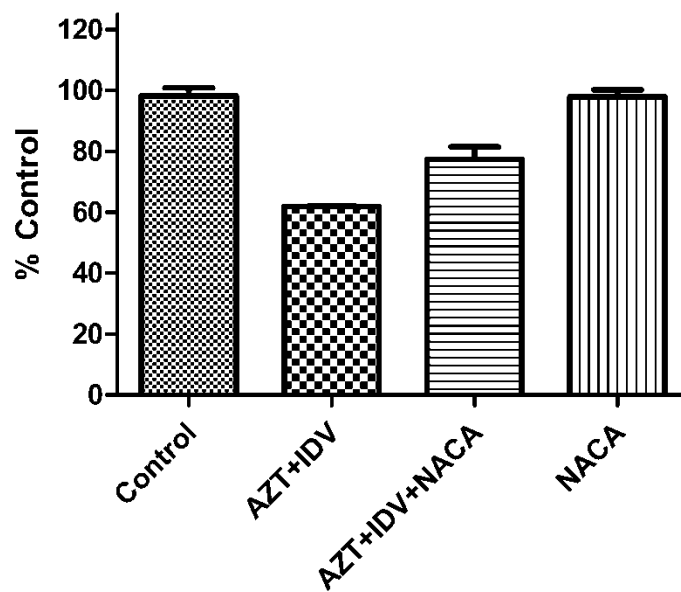
Figure 4.18. Effect of NACA on AZT+IDV induced cell death. Cells were pretreated with 2 mM NACA for 1 hr and then exposed to AZT+IDV (100 µM) for 72 hr. Viability was assessed using calcein AM fluorescent assay. Each value is the average of at least triplicate values with standard error mean bars (Mean±SEM; n=5).
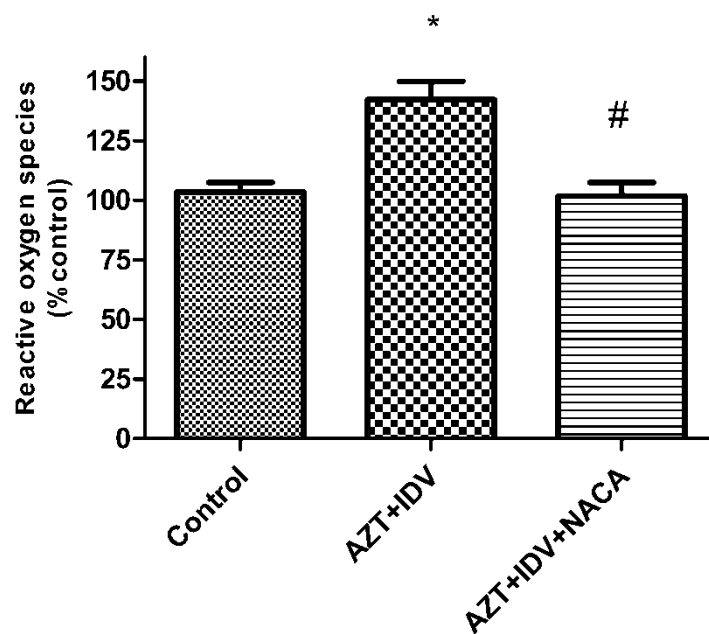
Figure 4.19. Effect of NACA on AZT+IDV induced ROS production. Cells were pretreated with 2 mM NACA for 1 hr and then exposed to AZT+IDV (100 µM) for 72 hr. Results are expressed as mean percent controls (Mean± SEM; n=4). * Statistical differences (p<0.05) as compared to untreated control. # Statistical differences (p<0.05) as compared to AZT + IDV treated control.
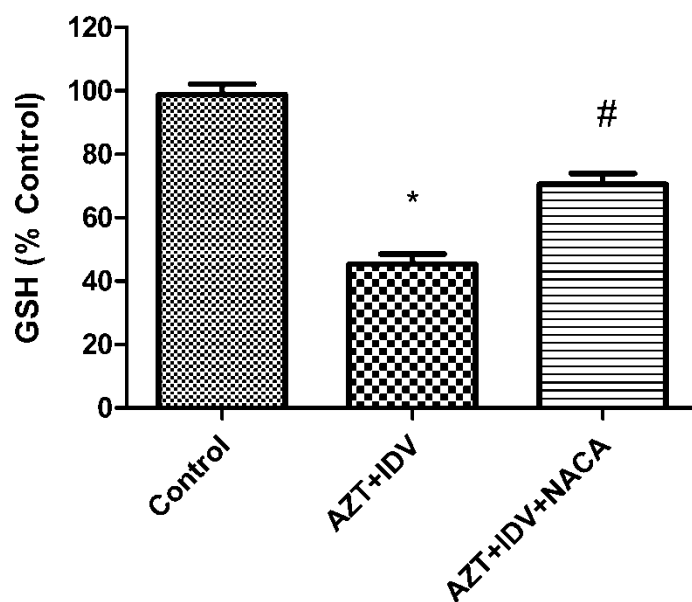
Figure 4.20. Effect of NACA on GSH levels in AZT+IDV treated cells. hCMEC/D3 cells were pretreated with 2 mM NACA for 1 hr and then exposed to AZT+IDV (100 µM) for 72 hr. Results are expressed as mean percent controls (Mean± SEM; n=4). * Statistical differences (p<0.05) as compared to untreated control. # Statistical difference (p<0.05) compared to AZT+IDV treated group.

5. *INVIVO* EXPERIMENTS

5.1 MATERIALS AND METHODS

5.1.1 Materials. F344 rats (normal and HIV-1 transgenic) were obtained from Harlan Laboratories (Indianapolis, IN). N-acetylcysteine amide was provided by Dr. Glenn Goldstein (David Pharmaceuticals, NewYork, NY, USA). N-(1-pyrenyl)-maleimide (NPM) was purchased from Sigma (St. Louis, MO). High-performance liquid chromatography (HPLC) grade solvents were purchased from Fisher Scientific (Fair Lawn, NJ). Antiretroviral drugs (ART), AZT and IDV were a gift from the National Institutes of Health AIDS Research and Reference Reagent Program. All other chemicals were purchased from Sigma (St. Louis, MO), unless stated otherwise.

**5.1.2. Animal Experiments.** Male F344 normal and HIV-1 transgenic (Tg) rats (200-250 g, 3 months old) were housed in a controlled temperature (20–23 ^{0}C) and controlled-humidity (~55%), in an animal facility, with a 12 h light and dark cycle. The animals had unlimited access to rodent chow and water, and were utilized after 1week of acclimatization. All animal procedures were conducted under an animal protocol approved by the Institutional Animal Care and Use Committee of the Missouri University of Science and Technology. The normal rats were divided into control and NACA control. HIV Tg rats were classified as experimental group. The HIV Tg rats in the experimental group further were divided into four major groups ($n = 4$ each): HIV group, HIV+ART, HIV+ NACA and HIV+ ART +NACA. All animals in the control and experimental groups were injected intraperitoneally (i.p) with either saline or NACA (500 mg/kg body weight), 30 min before exposure to ART drugs. The animals in the

respective experimental group were injected i.p with ART drugs (AZT+IDV, each

15mg/kg body weight for 10 days (Jiang et al., 2009). The rats were sacrificed 24 h after

the last exposure by urethane injection. All rats were weighed at the beginning and at the

end of the study. Following sacrifice, the brains were harvested and divided into two

parts, and the first half were placed in a cold stock buffer (25 mM HEPES, 1% dextran in

minimum essential medium) (Gibco BRL, Grand Island, N.Y.), at pH 7.4 on ice and the

remaining tissue was stored in an antioxidant buffer [8.6mM sodium phosphate dibasic

(Na_2HPO4), 26.6 mM sodium phosphate monobasic (NaH_2PO4), 50 µM

butylhydroxytoluene (BHT), 10mM aminotriazole, 0.1mM diethyltriaminepentaacetic

acid (DTPA)] at $-80\,^{0}C$ for further analysis.

5.1.3 Isolation of Brain Microvessels. Microvascular endothelial cells were

isolated using an established protocol (Wu et al., 2003). Briefly, brain tissues from rats

were homogenized in cold stock buffer (25 mM HEPES, 1% dextran in minimum

essential medium) (Gibco BRL, Grand Island, N.Y.), at pH 7.4 on ice. The homogenates

were then filtered through a series of nylon mesh membranes, after which they were

mixed with an equal volume of 40% dextran in stock buffer, and centrifuged at $5,000 \times g$

for 15 min at 4°C. The pellet obtained is re-suspended in a stock buffer and filtered

through a 25-µm pore-size nylon mesh membrane (Bio-Design, Carmel, NY). The micro-

vessels were then washed from the surface of the membrane with the stock buffer,

collected, and centrifuged at $5,000 \times g$ for 15 min at 4°C, after which they were re-

suspended in an incubation buffer [129 mM NaCl, 2.5 mM KCl, 7.4 mM Na_2HPO4,

1.3 mM KH_2PO4, 0.63 mM $CaCl_2$, 0.74 mM $MgSO_4$, 5.3 mM glucose, 0.1 mM ascorbic

acid (pH 7.4)], with a small aliquot being reserved for verification of an enriched micro-

vessel preparation by light microscopy. About 97.5% of the cells isolated were capillary endothelial cells, 1.6% were fibroblast-like cells, and 0.9% were erythrocytes. There were no glias, neurons, synaptosomes, or synaptic complexes, although there were some other membrane profiles and myelin fragments.

5.1.4. Determination of Glutathione (GSH) Levels. The levels of GSH in the BBB microvessels and brain were determined by RP-HPLC, according to the method developed in our laboratory (Winters et al., 1995). The HPLC system (Thermo Electron Corporation) consisted of a Finnigan Spectra System vacuum membrane degasser (model SCM1000), a gradient pump (model P2000), autosampler (model AS3000), and a fluorescence detector (model FL3000) with λex=330 nm and λem=376 nm. The HPLC column used was a Reliasil ODS-1 C_{18} column (5-μm packing material) with 250$\times$4.6 mm i.d (Column Engineering, Ontario, CA). The mobile phase (70% acetonitrile and 30% water) was adjusted to a pH of 2 with acetic acid and o-phosphoric acid. The NPM derivatives of GSH were eluted from the column isocratically at a flow rate of 1 ml/min. The microvessel pellets or brain tissues obtained were homogenized in 1 ml of serine borate buffer (SBB,100 mM Tris buffer containing 10 mM borate and 5 mM serine with 1 mM diethylene triaminepentacetic acid; Ph=7.4), centrifuged, and 250 μl of the supernatants were added to 750 μl of 1 mM NPM. The resulting solution was incubated at room temperature for 5 min, and the reaction was stopped by adding 10 μl of 2N HCl. The samples were then filtered through a 0.45 μm filter and injected into the HPLC system.

5.1.5. Determination of Malondialdehyde (MDA). The MDA levels were determined according to the method described elsewhere (Draper et al). Briefly, 550 μl of 5% trichloroacetic acid (TCA) and 100 μl of 500 ppm butylated hydroxytoluene (BHT) in methanol was added to 350 μl of the BBB microvessel or brain homogenates, and boiled for 30 min in a water bath. After cooling on ice, the mixtures were centrifuged, and the supernatant was collected and mixed 1:1 with saturated thiobarbituric acid (TBA). The mixture was again heated in a water bath for 30 min, followed by cooling on ice. 500 μl of the mixture was extracted with 1 ml of n-butanol and centrifuged to facilitate the separation of phases. The resulting organic layers first filtered through 0.45 μm filters and then injected into the HPLC system (Shimadzu, US), which consisted of a pump (model LC-6A), a Rheodyne injection valve and a fluorescence detector (model RF 535). The column was a 100×4.6 mm i.d C_{18} column (3 μm packing material, Astec, Bellefonte, PA). The mobile phase used contained 69.4% sodium phosphate buffer, 30% acetonitrile, and 0.6% tetrahydrofuran. The fluorescent product was monitored at λex= 515 nm and λem= 550 nm. Malondialdehyde bis (dimethyl acetal), which gives malondialdehyde on acid treatment, was used as a standard.

5.1.6. Measurement of Superoxide Levels. BBB microvessels were suspended in PBS, pH 7.2, containing 100 μg/ml bovine serum albumin and protease inhibitor cocktail (EDTA free complete protease mix; Roche Diagnostics, Indianapolis, IN). Reduced streptolysin O (5 units/ml; Sigma Aldrich) was added, and the mixture was incubated for 10 min at 37 °C (O'brien et al., 2009). The permeabilized cells were chilled to 4 °C, harvested by centrifugation, and washed with phosphate buffer, pH 7.2. To measure superoxide production, brain microvessels were resuspended in duplicate tubes,

with and without 200 units of SOD, containing 30 mM of 3-(N-morpholino)

propanesulfonic acid (MOPS (pH 7.2), 100 μM flavin adenine dinucleotide (FAD), and

100 μM oxidized cytochrome *c*, incubated at room temperature for 5 min, and

nicotinamide adenine dinucleotide phosphate (NADPH) added to a final concentration of

200 μM. The change in optical density at 550 nm was recorded every 5 min for 1 hr. At

the conclusion of the experiment, cells were lysed in 20 mM HEPES buffer containing

1% Triton X-100, and the protein was quantitated using the biorad protein assay.

Superoxide production was expressed as SOD-inhibitable cytochrome *c*

reduction/min/mg protein.

5.1.7. Measurement of NADPH Oxidase Activity. NADPH oxidase activity was

measured in brain using the lucigenin assay. Briefly, frozen brain samples were

homogenized in protease inhibitor-containing buffer at 4°C, and then subjected to

differential centrifugation to isolate purified cell membranes (obtained after sequential

centrifugations of 1300 x g to remove nuclei, 13,000 x g to remove mitochondria).

Membrane samples were then incubated with 5 μM lucigenin and 100 μM NADPH, and

NADPH oxidase activity was measured immediately using a luminescence plate reader at

37°C. To eliminate the background level of luminescence, membrane fractions of the

samples were also incubated in the presence of 1 μM diphenyl iodonium chloride (DPI),

a broad-spectrum flavin oxidase inhibitor.

5.1.8. Measurement of Nitrite Levels in the Brain. Nitrite levels in the BBB

microvessels were determined using a commercially available kit from Cayman Chemical

Company (Ann Arbor, MI). Briefly, this assay measures the nitrite concentration in two-

steps. The first step involves the conversion of nitrate to nitrite using nitrate reductase, and the second step converts the nitrite into a deep purple azo compound using the greiss reagent. Photometric determination of the absorption at 540 nm accurately determines the NO_2^- concentration.

5.1.9. Determination of Protein. Protein levels of the cell samples were measured by the Bradford method. Concentrated Coomassie Blue (Bio-Rad, Hercules, CA) was diluted 1:5 (v/v) with distilled water. 20 μl of the diluted cell homogenate was added to 1.5 ml of this diluted dye, and absorbance was measured at 595 nm using a UV spectrophotometer (Shimadzu Scientific Instruments, Columbia, MD). Bovine serum albumin (BSA) was used as the protein standard.

5.1.10. Statistical Analysis. Group comparisons were performed using the one-way analysis of variance (ANOVA) test and the TUKEYS post hoc test. Statistical analyses were made using GraphPad Prism 5.01 (GraphPad Software Inc., La Jolla, CA). Statistical significance was set at $p < 0.05$.

5.2. *IN VIVO* RESULTS

5.2.1. Changes in Glutathione Levels of Brain Microvessels and Brain. Table 5.1 shows the effect of viral proteins and ART drugs on GSH levels in blood-brain barrier. Compared to the controls, the HIV treated animals had a decrease (~ 3 fold) in the GSH levels in their blood brain barrier. A significant and drastic decrease (~ 6 fold) in the levels of GSH was observed in HIV transgenic animals treated with ART drugs when compared to controls. In this study, animals treated with ART also experienced a ~

1.5 fold decrease in GSH levels, as compared to the HIV group. Animals pretreated with NACA in both the HIV and HIV +ART groups showed an increase in GSH levels.

Evaluation of GSH levels in the brains of HIV transgenic animals and ART treated group are shown in Table 5.1. Compared to control, the HIV transgenic animals had a significantly lower level of GSH. Similarly, the HIV+ART group also had decreased levels of GSH in relation to control. There was no significant difference observed between the HIV and ART treated HIV group. Treatment with NACA elevated the GSH to a level similar to that of control group in both the HIV and ART treated group. These results suggest that viral proteins induce oxidative stress by decreasing the levels of GSH and these effects appear to be more potentiated with concomitant use of ART drugs. These outcomes also indicate the potent antioxidant ability of NACA to reverse these effects and replenish GSH in oxidatively challenged cells.

5.2.2. Effect of HIV Proteins and ART on MDA Levels in Brain. A significant increase in the level of MDA was observed in the brain tissue of HIV transgenic animals, as compared to those of the control and the NACA-alone treated group. HIV Tg animals treated with ART had a higher MDA levels than those of the control, but were similar to those of HIV group (Table 5.2). However, animals in the HIV group, pre-treated with NACA, had significantly lower MDA level than those of the untreated group, indicating that NACA was protecting the animals from oxidative stress-induced damage. Also animals in the HIV+ART group had lower levels of MDA than those of the control group, but similar to those of NACA group.

5.2.3. NADPH Oxidase Activity. The NADPH oxidase, a membrane-bound enzyme complex, normally generates superoxide by electrons by transferring electrons from NADPH inside the cell across the membrane and coupling these to molecular oxygen to produce the superoxide radical (O_2^{*-}). Figure 5.1 shows that, compared to the controls, HIV and HIV+ART treated animals experienced a significant increase in the NADPH oxidase activity in the brain. Pretreatment of the HIV+ART treated animals with NACA significantly decreased the NADPH oxidase activity, indicating that NADPH oxidase activation might be one of the reasons for increased oxidative stress in these animals.

5.2.4. Effect of ART Drugs on Superoxide levels in BBB. Several studies have shown that NADPH oxidase is the most important source of superoxide anion in phagocytic and vascular cells. Increase in NADPH oxidase activity is correlated to increase in superoxide levels. Figure 5.2 displays the results of superoxide levels in blood-brain barrier. Although superoxide levels were unchanged in HIV Tg group, ART treated HIV group showed a significant (~6 fold) increase in superoxide levels ($p<0.05$). Pretreatment with NACA decreased the superoxide levels to remarkably lower levels, similar to that of control group ($p<0.05$). These results indicate NADPH oxidase enzyme may be involved in the oxidative stress induced by ART drug in BBB.

5.2.5. Nitrite Levels in Brain after AZT+IDV Treatment. Activation of NADPH oxidase enzyme results in an increase in the superoxide levels (O_2^{--}). Superoxide radicals react with nitric oxide (NO·), which gives rise to highly pro-oxidant peroxynitrite ($ONOO^-$). This compound triggers the formation of nitrotyrosine residues (Ntyr), which

provides a tissue marker for reactive nitrogen-related tissue damage. Figure 5.3 displays the increase in levels of nitrite in the brain samples of both HIV group as well as the ART drug treated HIV group. The increases in the nitrite levels in both groups were significantly different from control and the nitrite levels of brain were higher in ART treated group than HIV transgenic animals. There was significant decrease in nitrite levels of brain samples of NACA treated HIV+ART group. These results indicate the involvement of a convergent mechanism in BBB dysfunction and also show that NACA can alleviate some of the harmful effects of NADPH oxidase mediated injury.

Table 5.1. GSH levels in BBB and Brain of HIV-Tg rats. (GSH: nmoles/mg of protein). Results expressed as mean values (Mean±SEM; n=4). * Statistical differences (p<0.05) as compared to untreated control, ** (p<0.05) compared to HIV treated group, # (p<0.05) compared to HIV+ART treated group.

Groups	GSH	
	Brain microvessels	**Whole brain**
Control	5.7±0.6	15.1±1.6
NACA	3.2±0.5	16.4±5.0
HIV	1.6±0.1*	10.7±1.1*
HIV+NACA	2.2±0.1**	19.1±8.6
HIV+ART	0.9±0.1*	12.0±1.3*
HIV+ART+NACA	1.1±0.1	23.3±1.3[#]

Table 5.2. MDA levels in Brain of HIV-Tg rats. (MDA: nmoles/100mg of protein). *
Statistical differences (p<0.05) as compared to untreated control, ** (p<0.05) compared
to HIV treated group, # (p<0.05) compared to HIV+ART treated group (Mean±SEM;
n=4).

Groups	MDA
Control	67.0±3.7
NACA	55.9±2.6
HIV	78.1±3.8*
HIV+NACA	50.2±8.8**
HIV+ART	73.0±3.1*
HIV+ART+NACA	55.9±6.2[#]
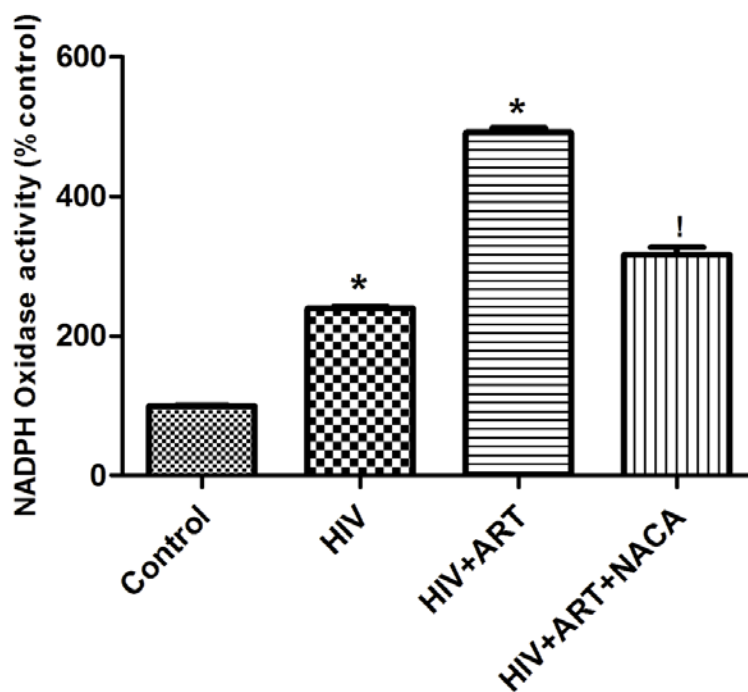
Figure 5.1. Effect of ART drugs and NACA on activity of NADPH oxidase. NADPH oxidase activity was measured in the brain of HIV-Tg animals treated with ART (AZT+IDV) drugs for 10 days. Animals in the NACA group pretreated with NACA 30 mins before ART drug injection. NADPH oxidase activity of the NACA alone and HIV+NACA treated group similar to that of the control (data not shown). Data: Mean±SEM; n=4. (*) indicates significantly different from the control, (!) significantly different from the HIV+ART treated group.
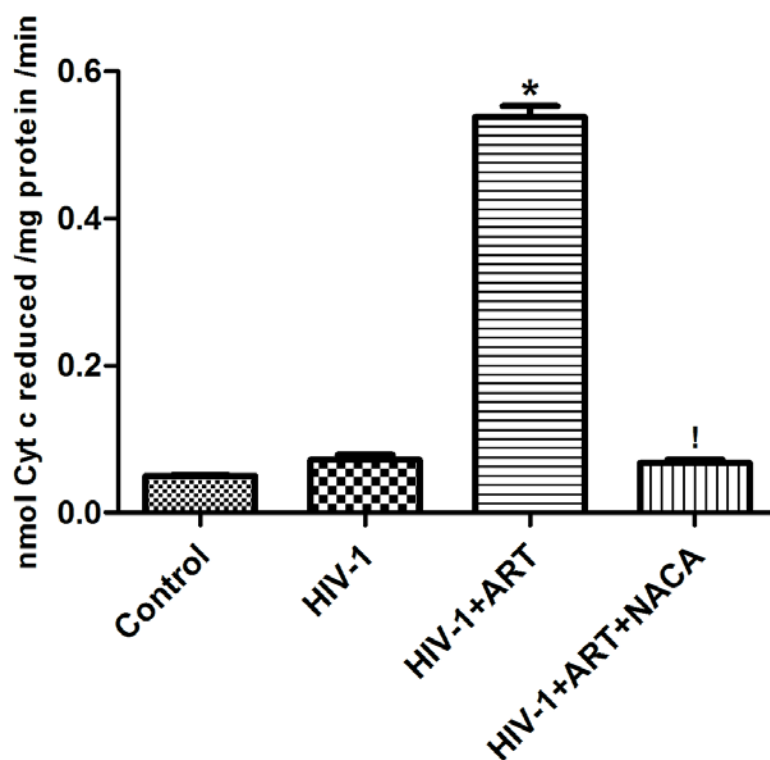
Figure 5.2. Effect of NACA on superoxide levels. Superoxide radical formation was measured in the BBB in the brain of HIV-Tg animals treated with ART drugs (AZT+IDV) drugs for 10 days. Animals in the NACA group pretreated with NACA 30 mins before ART drug injection. Superoxide radical formation of the NACA alone and HIV+NACA treated group similar to that of the control. Data: Mean±SEM; n=4. (*) indicates significantly different from the control, (!) significantly different from the HIV+ART treated group.
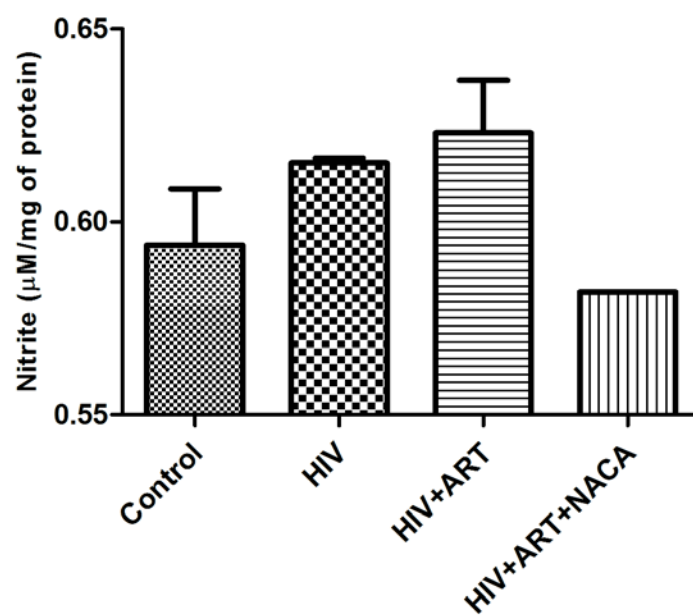
Fıgure 5.3. Effect of ART drugs and NACA on nitrite levels. Brain nitrite levels shown above. Results expressed as average of mean values (Mean±SEM; n=2).

6. DISCUSSION

6.1. *IN VITRO* RESULTS

The advent of HAART therapy has significantly revolutionized the treatment of AIDS by increasing the lifespan of HIV-infected individuals, and creating a decline in AIDS-related neurological disorders (Bell, 1998; Nath, 2002). Although HAART treatment has reduced the prevalence of opportunistic infections like cytomegalovirus and toxoplasmosis, the clinical impact of HAART toxicity on HIV-1-associated neurocognitive disorders is still controversial (Krebs et al., 2000). Most of the clinical studies report that cognitive impairment is still a significant clinical problem in HAART-treated patients (Dore et al., 1999). Although several *in vitro* studies have shown that HIV proteins and methamphetamine can cause dysfunction in the BBB, the effect of HAART drugs on the BBB endothelial cells and its role in exacerbating HAND are not yet known. In this study, we have used the combination of AZT and IDV, one of the most commonly recommended HAART regimens, to elucidate their role in free radical generation and mitochondrial dysfunction mediated endothelial cell death.

Here, we present evidence that HAART drugs are toxic to BBB endothelial cells in a dose-dependent manner (Figure 4.1). We suggest that the high AZT and IDV concentrations found to be active in our studies can be considered relevant. AZT + IDV is used for the treatment of HIV-infected AIDS patients at doses of about 500–1500 mg daily for a long survival period. The concentrations used in our experiments are achieved at serum levels after oral administration (Collier et al., 2003). Endothelial cells exposed to individual drugs showed that AZT was more toxic than IDV. AZT, a nucleoside reverse transcriptase inhibitor, has been shown to decrease the levels of mitochondrial

DNA *in vivo* and clinically by inhibiting γ-DNA polymerase (Simpson et al., 1989; Lewis et al., 1992). The decrease in mtDNA inhibits the synthesis of adequate proteins for oxidative phosphorylation (OXPHOS). A subsequent energy loss and increase in production of reactive oxygen species (ROS) has been reported in other studies involving HAART treatment (Mondal et al., 2004). Our data concurs with those studies, as a significant, concentration-dependent increase in total ROS was also observed in our study, indicating an increase in the oxidative stress in response to the treatment (Figure 4.5).

One of the important effects of oxidative stress and free radical generation is decreased levels of cellular antioxidants. GSH (γ-glutamyl-cysteinyl-glycine), a thiol antioxidant in cells, is mainly responsible for maintaining cellular redox status in endothelial cells. GSH scavenges free radicals and hydrogen peroxide, and neutralizes toxic metabolites by condensing with them both enzymatically and nonenzymatically (Meister, 1995). Long-term AZT treatment has been shown to induce oxidative damage and deplete GSH in rats treated acutely and in cell cultures (Szabados et al., 1999). We observed a dose-dependent decrease in GSH levels after HAART treatment suggesting that AZT + IDV induced ROS production with subsequent decreases in GSH levels (Figure 4.6). AZT + IDV may have caused an increase in levels of hydroperoxides that exceeded the metabolic capabilities of the glutathione system to maintain glutathione in the reduced form. In fact, mitochondria are highly dependent on glutathione to detoxify ROS and prevent oxidative damage (Lewis et al., 1995).

A decrease in GSH and an increase in ROS set off a cascade of further oxidative damage. An important target of oxidative damage is brain microvessel endothelial cells

because they are rich in polyunsaturated fatty acids (PUFAs). ROS attacks double bonds

in PUFAs, thereby degrading the lipids and generating MDA as by product. MDA is a

widely used oxidative stress parameter, reacting with deoxyadenosine and

deoxyguanosine to form mutagenic DNA adducts (Marnett, 1999). Studies have shown

that AZT treated mice have higher levels of plasma MDA, as compared to control mice

(Garcia et al., 2007).Our results also indicated that AZT + IDV treatment increased the

levels of lipid peroxidation metabolites because of oxidative damage (Fig. 4.7).

The predominant enzymatic mechanisms that regulate intracellular H_2O_2 levels

are mediated by catalase and glutathione peroxidase. In the current study, catalase

activity of hCMEC/D3cells after exposure to AZT+IDV was measured by following the

disappearance of H_2O_2. As indicated in figure (4.8), a dose dependent decrease in catalase

activity was seen after 72 hr exposure to AZT+IDV. The ability of AZT+IDV to reduce

catalase activity has been shown before in other models, such as the human umbilical

endothelial cell line, HUVEC. Transduction with the mitochondria-targeted catalase

(mCAT) was more effective than cytoplasmic catalase in inhibiting the ROS and 8-

isoprostane (8-iso-PGF2alpha) produced after treatment with either AZT or indinavir

(Jiang et al., 2007). Similarly transgenic animals overexpressing mCAT treated with AZT

were protected from cardiac dysfunction (Kohler et al., 2009). It is so far poorly

understood through which mechanisms AZT and IDV affect the function of catalase.

However it is thought that tyrosyl radical in catalase enzyme is involved in the in the

catalytic activity of the enzyme (Ivancich et al., 1997; Chouchane et al, 2002). Nitration

or reaction of free radicals with this tyrosine residue could lead to inactivation of the

enzyme. Other studies have reported that phosphorylation of the tyrosine residue on

catalase may lead to decreased activity of catalase enzyme (Zhang et al., 2005; Suarez et al., 2009).

Mitochondria are logical targets for oxidative stress, based on their ability to generate free radicals, and may be primarily involved in oxidative stress associated with AIDS treatment. Under physiological conditions, reactive oxygen species (ROS) are produced mainly by the mitochondria during OXPHOS, as electrons travel through the electron transport chain (ETC). During OXPHOS, electrons leak out of the ETC and result in the formation of superoxide instead of water. Superoxide is generated at complex I (NADH dehydrognase) and complex III (ubiquinone Q-cytochrome b). Any alteration in redox status of these complexes results in an excessive production of superoxide radical (Boveris et al., 1973). Mitochondrial hydrogen peroxide is also rapidly formed from superoxide by dismutation or by mitochondrial manganese superoxide dismutase. Hydroxyl radicals are known to form at sites where superoxide and hydrogen peroxide are formed in mitochondria (Taylor et al., 1995). The free radicals generated can act on mitochondrial proteins, lipids, and even mtDNA, thereby altering the electrochemical gradient across the mitochondria resulting in mitochondrial dysfunction (Lin et al., 2006). An electrochemical gradient across mitochondrial inner membrane or mitochondrial membrane potential ($\Delta\Psi$m) is important for mitochondrial electron transport and energy metabolism. A decrease in $\Delta\Psi$m after treatment was detected and assessed in our studies by using fluorescent microscopy. In addition to this, we also observed a dose-dependent decrease in ATP levels after treatment. Loss of $\Delta\Psi$m interferes with the production of ATP, the cell's main source of energy, because mitochondria must have an electrochemical gradient to provide the driving force for ATP

production. Decreases in $\Delta\Psi$m and ATP levels seen in our study are consistent with disrupted mitochondrial function.

To determine the oxidative stress effect of AZT+IDV, the expression of MnSOD expression was evaluated. Results from 50 µM indeed support the fact, as seen by increased expression of MnSOD. In support to our results, various other studies have reported that a mild to moderate increase in oxidative stress increased MnSOD expression in various cell types (Li et al., 2010; Liu et al., 2010). Higher or overwhelming oxidative stress tends to decrease the expression of MnSOD levels as seen from results in 200 µM treated groups (Chaudauri et al., 2010).

Reactive oxygen and nitrogen species, decreased mitochondrial membrane potential, and oxidation of pyridine nucleotides and glutathione all promote mitochondrial damage and the onset of a phenomenon known as mitochondrial permeability transition (MPT). MPT is a sudden increase in the permeability of the inner mitochondrial membrane, loss of $\Delta\Psi$m, uncoupling of oxidative phosphorylation, mitochondrial swelling, and the release of intramitochondrial ions through the mitochondrial membrane transition pore (MPTP) (Lemasters et al., 1998). Mitochondrial permeability transition (MPT), is recognized as an initiating phenomenon, important for both necrosis and apoptosis (Lemasters et al., 1998). Swelling of the mitochondria due to increased permeability ruptures the outer membrane of the mitochondria releasing the cytochrome *c* into the cytoplasm. Cytochrome *c* can, in turn, cause apoptosis of cells by activating pro-apoptotic factors (Skulachev, 1998). Endothelial cell apoptosis has been demonstrated in an atherosclerotic lesion and has been considered a mechanism for atherogensis in HAART-treated patients (Barbaro et al., 2006). AZT treatment has

induced apoptosis in placental cells and parathyroid cancer cells (Falchetti et al., 2005).

Contrary to these and various other studies, AZT + IDV did not induce apoptosis at

therapeutic concentrations in primary human umbilical cells and various other studies

(Jiang et al., 2007). In addition to this, an emerging body of literature suggests that

protease inhibitors may also be anti-apoptotic by inhibiting calpain (Lichtner et al.,

2006). In view of this conflicting research, we tested whether AZT + IDV can induce

apoptosis in hCMEC/D3 cells. Cytchrome c and procaspase 3 levels were elevated in

cytosolic fractions of the treated groups when compared to those of the control groups.

To further ascertain that AZT + IDV treatment induced apoptosis, cells stained with an

AO/EB mixture were observed under a fluorescent microscope. Treated cells showed

changes in cellular morphology, including chromatin condensation, membrane blebbing,

and fragmented nuclei and apoptotic bodies. Results from both studies provided sufficient

support that AZT + IDV treated hCMEC/D3 cells were undergoing programmed cell

death.

Apoptosis can be triggered by many different stimuli, including engagement of

death receptors by cytokines (such as TNF-alpha and Fas ligand), toxins, and oxidative

stress. Early events in apoptosis include the release of cytochrome c (from mitochondria)

and calcium from endoplasmic reticulum in to the cytosol, which are necessary for

apoptosis. A small amount of cytochrome c released from mitochondria can bind to and

promote calcium conductance through inositol-1,4,5–triphosphate ($InsP_{3)}$ receptors in the

endoplasmic reticulum membrane. The released calcium then triggers a massive exodus

of cytochrome c from all mitochondria in the cell, thereby activating the caspases and

nuclease enzymes that finalize the apoptotic process (Boehning et al., 2003). Evidently,

calcium uptake into the mitochondria is secondary to an increase in the cytoplasmic calcium concentration as a stimulus for the massive release of cytochrome c. Results from our studies show that a calcium based mechanism may be involved in the extensive release of cytochrome c and the execution of cell death induced by an AZT + IDV combination in blood-brain vascular endothelial cells.

A noticeable decrease in trans-endothelial electrical resistance (TEER) and an increase in dextran permeability across the monolayer of endothelial cells provide evidence that HAART drugs induce gaps between endothelial cells. This is in agreement with results reported from previous studies (Fiala et al., 2000). Inflammatory mediators (histamine and thrombin) tend to increase centripetal tension and intercellular and matrix adhesion in the absence of a rise in cyclic adenine monophosphate. Thrombin triggers multiple signal pathways through activation of G proteins which can, in turn, activate phospholipase C. Activation leads to a series of signaling cascades, ultimately leading to protein kinase C activation. These signals lead to activation of multiple protein kinases and phosphorlyation of their target proteins, filamin, myosin light chain kinase (MLCK), and tight junction (TJ) proteins (Sansdoval et al., 2001). Phosphorylation of these target proteins induces interendothelial gaps and monocyte migration across the BBB models (Bogatcheve et al., 2002). Our data concurs with a previous study on endothelial cells, which showed that HAART drugs can induce gaps between endothelial cells.

Glutathione (L-γ-glutamyl-L-cysteinylglycine, GSH) is the most prevalent intra-cellular thiol in mammals. It is known to be involved either directly or indirectly in a number of biological phenomena, including protecting cells from harmful reactive oxygen intermediates (ROI), and acting as a coenzyme in several enzyme catalyzed

reactions. Although GSH by itself is poorly absorbed through cells and has high affinity for oxidation, various analogues of cysteine and GSH have been synthesized known to easily permeate cell. One such kind of analogue known to pass BBB and increase GSH levels is N-acetylcysteine amide (NACA). Although cytotoxicity in AZT+IDV treated cells was abolished, a slight increase in viability was observed in cells pretreated with NACA.

In order to comprehend the results, and further establish the antioxidant effects of NACA, the ROS levels in treated cells were evaluated. NACA completely decreased the ROS levels in the AZT+IDV treated group. These results agree with data reported from previous other studies, where NACA successfully inhibited the increase in free radicals (Penugonda et al., 2005) NACA is thought to increase GSH levels in cells, both by providing the important GSH precursor cysteine, and by reducing GSSG back to GSH by thiol disulfide exchange (Grinberg et al., 2005). According to figure 4.20 NACA appears, to replenish GSH levels, which may be useful in reversing some of deleterious effect of oxidative insults.

The ability of NACA to scavenge ROS and increase GSH levels without a significant effect on cell viability, as seen in our studies, has also been reported in previously reported studies of NACA (Rong et al., 2009). Moreover cells were only preinucbated with NACA in our studies for only 1 hr prior to 72 hr exposure with AZT+IDV. Further research needs to be done to develop an effective dosing protocol to efficiently establish the effects of NACA.

In summary, our results demonstrate that the HAART drug combination of AZT + IDV can induce cytotoxicity and alter the blood-brain endothelial cell functions.

Alteration of the endothelial functions is due to increased oxidative stress and lipid peroxidation. Our results also suggest that treatment with AZT + IDV leads to depolarization of membrane potential and energy loss, ultimately causing mitochondrial dysfunction. Furthermore, treated cells undergoing apoptosis and elevated intracellular calcium mediated the drug-induced apoptosis in our current study. Thus, treatment with HAART drug combinations may have to be used with caution in HIV-infected patients, although inclusion of antioxidants like NACA in HAART therapy may protect patients with HIV-1 associated neurocognitive disorders from drug-induced toxicity.

6.2. *IN VIVO* RESULTS

Vascular function is as essential as the heart beat, since it regulates blood pressure and thereby protects from hypertension and atherosclerosis in the long term. In addition, it maintains the function of the vessel walls as a blood-barrier in the brain and thereby prevents leukocyte infiltration as well as inflammatory processes in the vascular wall. Blood-brain barrier disruption has been implicated in numerous neurocognitive disorders. The role of HAART drugs in BBB disruption and the mechanism involved in this disruption is poorly understood in HAND. Our previous *in vitro* study with HAART drugs proved that AZT + IDV induced toxicity through an oxidative stress mediated mechanism in cell model of the BBB. Pretreatment with NACA abrogated some of the effects due to drug exposure in *in vitro* study. In addidition, an *in vivo* study was conducted to further understand the mechanism and implicate the oxidative stress role of HAART drugs in BBB disruption, and also to establish the protective role of thiol antioxidant NACA to protect against oxidative stress in HIV transgenic animals treated with HAART drugs.

Initially to elucidate the oxidative stress effect of viral proteins and antiretroviral drugs in the BBB and brain, GSH levels were measured in BBB microvessels as well as in the brain (Table 5.1). In the literature, a decrease in GSH levels has been connected to physiological processes such as aging and neurological disorders like schizophrenia, Alzheimer's disease, and epilepsy (Do et al., 2000; Gu et al., 1998; Mueller et al., 2001). Previous studies from our lab have reported that animals exposed to HIV viral proteins (gp120+Tat) had significant decreases in GSH levels in their brains as compared to controls. In our study we report similar results in the brain as well as the BBB, which indicate that viral proteins decrease GSH (Banerjee et al., 2010). The decrease in GSH is attributed to increase in oxidative stress in cell culture and in *in vivo* settings as well. Along with that, treatment with ART drugs also decrease GSH in the BBB and the brain. This result advocates our findings obtained in BBB cell model. NACA treatment in these animals replenished the thiol levels in both HIV and HIV+ART group. Decreased GSH may increase the susceptibility to free radical attack of cellular proteins and lipids resulting in MDA, an end product of lipid peroxidation. Our results in both the HIV and HIV group treated with ART drugs show an increase in MDA levels. Pretreatment with NACA decreased the levels of MDA in both the HIV and HIV+ART groups.

Various effects of HIV neuropathology in HAART-medicated patients have been reported, including severe white matter injury, extensive perivascular lymphocytic infiltration, and Aβ accumulation of AD-like lesions (Gray et al., 2003, 2005; Greene et al., 2005). Recent studies suggest that HAND prevalence is actually rising as the number of treated subjects with chronic HIV infection increases, despite HAART medication (Xu et al., 2009). Consequently, considering the link between chronic neuroinflammation,

neuronal/ synaptodenritic degeneration and Alzheimers disease, neuroinflammation is likely to play an important role in the pathogenesis of HAND by the killing of neurons through inflammatory mechanisms. ROS play a key role in inflammatory tissue destruction. The phagocyte NADPH oxidase is the best studied ROS-generating system. In the central nervous system, it is expressed in microglia in the brain and to a lesser extent in neurons. Indeed, there is emerging experimental evidence for a role of NADPH oxidase in Alzheimer's and cerebrovascular disease. Recently, six novel ROS-generating NADPH oxidases have been discovered (Sankarpandi et al., 1998; Bianca et al., 1999). Several of them are also expressed in the central nervous system. In this current study, we hypothesize a role of NADPH oxidases in neurocognitive disorders in HAART treated patients.

In addition to mitochondrial sources of ROS, $O_2^{\cdot-}$ can be derived from xanthine oxidase, NADPH oxidases, cyclooxygenases, lipoxygenases and uncoupled nitric oxide synthase. On the basis of experimental and clinical studies it has been proposed that NADPH oxidase is the predominant, $O_2^{\cdot-}$ producing enzyme in the context of oxidative stress. NADPH oxidase activation has also been implicated in loss of neuronal coupling.

According to figure 5.1 NADPH oxidase activities in both the HIV and ART-treated group appear to be elevated, with the latter showing a higher activity than former HIV group. To best of our knowledge we are the first to report the increase in NADPH oxidase activity in brain samples of ART treated HIV transgenic animals. NADPH oxidase activation has been also implicated in disruption of blood brain barrier following stroke and in apoptosis (Kahles et al., 2007). Administration of NACA appears to have

alleviated some of the NADPH oxidase activity. Although the specific inhibitory mechanism involved cannot be explained at this juncture.

Activation of NADPH oxidase enzyme results in transport of electrons from NADPH to molecular oxygen resulting in formation of superoxide. In order to support our earlier assumption and results of NADPH oxidase activation, we measured the superoxide levels. Although the HIV treated group did not show any increase in $O_2^{\cdot-}$ when compared to control, ART treated HIV group showed a massive increase in $O_2^{\cdot-}$ levels. Studies with ritonavir showed an increased NADPH oxidase activity in porcine arteries (Chai et al., 2005). Wang et al have shown that superoxide anion is significantly increased in porcine coronory arteries treated with ritonavir and amprenavir. Furthermore, they showed that indinavir and AZT- treated porcine arteries also had a significant increase in superoxide levels when compared to control (Wang et al., 2009; Jiang et al., 2010). Treatment with NACA decreased the superoxide levels in the ART treated HIV group (Figure 5.2). This effect can be explained based on the thiol group (-SH) group in NACA. Thiols react with free radicals by quenching the free radicals and, in turn losing proton forming thiyl radicals, which undergo a self-quenching process by forming a disulfide bond.

NADPH oxidase-derived superoxide reacts with $NO^{\cdot}$ to form peroxynitrite ($ONOO^{-}$) that is toxic. The highly reactive peroxynitrite has been implicated in the death of cultured neurons and oligodendrocyte progenitors (Scott et al., 2003). Tyrosine nitration, a marker of $ONOO^{-}$ activity, has been correlated with tissue damages in human neuropathologies such as multiple sclerosis, ALS, and Parkinson's and Alzheimer's diseases, as well as in animal models of these diseases, including LPS-triggered

neuroinflammation (Cheret et al., 2008). Our results (shown in Figure 5.3) indicate an increase in the levels of nitrite formation in ART treated HIV group as a result of higher superoxide levels generation mediated by NADPH oxidase. It is also interesting that the ART treated group had a greater increase in nitrite levels when compared HIV groups indicating that ART may be potentiating NADPH oxidase activity in HIV transgenic animals. Treatment with NACA significantly reduced the nitrite levels in ART +HIV group. Peroxynitrite reacts with the thiol group producing the unstable sulphenic acid, which in turn reacts with another thiol yielding the disulphide by a two electron oxidation pathway. One-electron oxidation pathway is also believed involved in reducing peroxynitrite levels. Peroxynitrous acid, or a secondary species derived from it, reacts with the thiol producing the thiyl radical. The latter can dimerize to the disulphide, or can react with oxygen to produce the peroxyl radical or with the thiolate yielding the disulphide radical anion (Quijano et al., 1997).

A proposed convergent mechanism based upon our *in vitro and in vivo* results, involved in blood-brain endothelial dysfunction as illustrated in Figure 6.1. HAART drugs may induce oxidative stress and mitochondrial dysfunction by increasing reactive oxygen species. These ROS may, in turn cause a decrease in GSH and increase in an MDA levels. Changes in these parameters may also result in apoptosis and endothelial dysfunction. It is also possible that HAART drugs may activate NADPH oxidase enzyme, thereby increasing superoxide production, which, in turn may lead to peroxynitrite radical generation. Nitration of proteins and enzymes by $ONOO^-$ may lead to further deleterious signaling cascade, resulting in BBB endothelial dysfunction and neurodegeneration in the brain and neurocognitive disorders in HAART- treated HIV subjects.
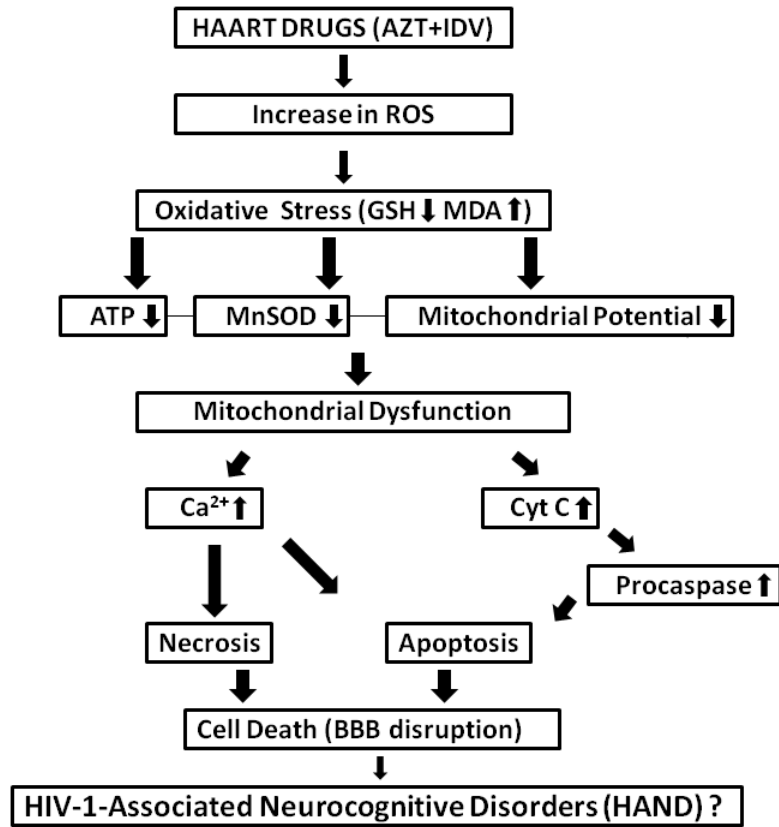
Figure 6.1. Schematic illustration of proposed mechanism for BBB dysfunction.

7. CONCLUSION

HIV-1 associated neurocognitive disorders are a still a significant health concern in HIV patients treated with antiretroviral therapy. Although HAART treatment has resulted in decreased mortality, the negative impact of therapy resulted in endothelial dysfunction related disorders like cardiovascular diseases. However, their effect on BBB and brain has not been studied in relation to neurocognitive disorders. Our study attempted to evaluate the effect of an antiretroviral drug combination of AZT and IDV on the BBB and brain.

Findings from our *in vitro* studies with HAART drugs (AZT+IDV) indicate that prolonged use of antiretroviral drugs may alter the function of the BBB. These potential toxic effects appear to be manifested through the dysfunction of the mitochondria and increase in oxidative stress. Our results from *in vivo* studies demonstrate that an alternate pathway involving reactive nitrogen species (RNS) may take part in signaling cascade of BBB disruption and neuronal degeneration in the brain. The protective effects of NACA were also shown in reducing the oxidative stress mediated effects of the AZT and IDV combination. The antioxidant effects of NACA against RNS were also prominent in ART -treated HIV transgenic rats. The increases in oxidative stress and NADPH oxidase activity in the BBB and brain is of particular concern in ART- treated groups and may signify their ability to potentiate the degenerative effect of viral proteins. No neurodegenerative markers were studied in this part of research, so the role of ART drugs in HAND is still unclear and needs further in depth investigation. The inclusion of thiol antioxidants like NACA, with the ability to cross the BBB, may prove beneficial in delaying or inhibiting some of the symptoms of neurocognitive disorder.

BIBLIOGRAPHY

Abbott NJ . Inflammatory mediators and modulation of blood –brain barrier permeability. Cellular and Molecular Neurobiology (2000), 20, pp. 131–147.

Aebi H. Catalase in vitro. Methods in Enzymology (1984), 105, pp. 121-6.

Agarwal R, Gupta A, Shukla GS. Developmental pattern of reactive oxygen species generation and antioxidative defense machinery in rat cerebral microvessels. International Journal of Developmental Neuroscience (1999), 17, pp. 673–679.

Aksenov MY, Aksenova MV, Mactutus CF, Booze RM. HIV-1 protein-mediated amyloidogenesis in rat hippocampal cell cultures. Neuroscience Letters, (2010) 475(3), pp. 174-8.

Annunziata P, Cioni C, Toneatto S, Paccagnini E. HIV-1 gp120 increases the permeability of rat brain endothelium cultures by a mechanism involving substance P. AIDS (1998), 12, pp. 2377–2385.

Annunziato L, Amoroso S, Pannaccione A, Cataldi M, Pignataro G, D'Alessio A, Sirabella R, Secondo A, Sibaud L, Di Renzo GF. Apoptosis induced in neuronal cells by oxidative stress: role played by caspases and intracellular calcium ions. Toxicology Letters (2003), 139(2-3), pp. 125-33.

Ates B, Abraham L, Ercal N. Antioxidant and free radical scavenging properties of N-acetylcysteine amide (NACA) and comparison with N-acetylcysteine (NAC). Free Radical Research (2008), 42(4), pp. 372-7.

Atlas D, Melamed E, Offen D: Brain targeted low molecular weight hydrophobic antioxidant compounds. U.S. Patent No. 5,874,468. 1999.

Bahat-Stroomza M, Gilgun-Sherki Y, Offen D, Panet H, Saada A, Krool-Galron N, Barzilai A, Atlas D, Melamed Epp. A novel thiol antioxidant that crosses the blood brain barrier protects dopaminergic neurons in experimental models of Parkinson's disease. European Journal of. Neuroscience (2005), 21(3), pp. 637-646.

Banerjee A, Zhang X, Manda KR, Banks WA, Ercal N. HIV proteins (gp120 and Tat) and methamphetamine in oxidative stress-induced damage in the brain: potential role of the thiol antioxidant N-acetylcysteine amide. Free Radical Biology Medicine (2010), 48, pp. 1388-98.

Banks WA, Freed EO, Wolf KM, Robinson SM. Transport of human immune deficiency virus type 1 pseudoviruses across the blood–brain barrier: role of envelope proteins and adsorptive endocytosis. Journal of Virology (2001), 75, pp. 4681–4691.

Bartov O, Sultana R, Butterfield DA, Atlas Dpp. Low molecular weight thiol amides attenuate MAPK activity and protect primary neurons from Abeta(1-42) toxicity. Brain Research (2006), 1069(1), pp. 198-206.

Behrens G, Dejam A, Schmidt H, Balks HJ, Brabant G, Körner T, Stoll M, Schmidt RE. Impaired glucose tolerance, beta cell function and lipid metabolism in HIV patients under treatment with protease inhibitors. AIDS (1999), 13(10), pp. F63-70.

Bell JE. The neuropathology of adult HIV infection. Reviews in Neurology (1998), 154(12), pp. 816-29.

Bellizzi MJ, Lu SM, Gelbard HA. Protecting the synapse: evidence for a rational strategy to treat HIV-1 associated neurologic disease. Journal of Neuroimmune Pharmacology (2006), 1, pp. 20–31.

Bianca VD, Dusi S, Bianchini E, Dal Pra` I, Rossi F. beta-amyloid activates the O-2 forming NADPH oxidase in microglia, monocytes, and neutrophils. A possible inflammatory mechanism of neuronal damage in Alzheimer's disease. Journal of Biological Chemistry (1999), 274, pp. 15493–15499.

Block, JH, Beale JM. Antiviral Agents, Wilson and Gisvold's Textbook of Organic Medicinal and Pharmaceutical Chemistry, 11th ed; Lippincott Williams & Wilkins: Maryland, 2004, pp. 379.

Boehning D, Patterson RL, Sedaghat L, Glebhova NO, Kurosaki T, Synder SH. Cytochrome c binds to inositol (1,4,5) triphosphate receptors,amplifying calcium-dependent apoptosis. Nature Cellular Biology (2003), 5, pp. 1051-61.

Bogatcheva NV, Garcia, JG, Verin AD. Role of tyrosine kinase signaling in endothe -lial cell barrier regulation. Vascular Pharmacology (2002), 39, pp. 201-12.

Boveris A, Chance B. The mitochondrial generation of hydrogen peroxide. General properties and effect of hyperbaric oxygen. Journal of Biochemistry (1973), 134, pp. 707–716.

Bradford MM. A rapid and sensitive method for the quantitation of microgram quantities of protein utilizing the principle of protein–dye binding. Analytical Biochemistry, (1976), 72, pp. 248– 254.

Caron M, Auclair M, Vigouroux C. Human lipodystrophies linked to mutations in A-type lamins and to HIV protease inhibitor therapy are both associated with prelamin A accumulation, oxidative stress and premature cellular senescence. Cell Death and Differentiation, (2007), 14, pp. 1759–1767.

Carr A, Samaras K, Thorisdottir A, Kaufmann GR, Chisholm DJ, Cooper DA. Diagnosis, prediction, and natural course of HIV-1 protease-inhibitor-associated lipodystrophy, hyperlipidaemia, and diabetes mellitus: a cohort study. Lancet, (1999), 353, pp. 2093-9.

Castellon SA, Hinkin CH, Wood S, Yarema KT. Apathy, depression, and cognitive performance in HIV-1 infection. Journal of Neuropsychiatry and Clinical Neuroscience (1998), 10, pp. 320-329.

Chai H, Yang H, Yan S, Li M, Lin PH, Lumsden AB, Yao Q, Chen C. Effects of 5 HIV protease inhibitors on vasomotor function and superoxide anion production in porcine coronary arteries. Journal of Acquired Immune Deficiency Syndrome 2005, 40(1), pp. 12-19.

Chéret C, Gervais A, Lelli A, Mallat M. Neurotoxic activation of microglia is promoted by a nox1-dependent NADPH oxidase. Journal of Neuroscience (2008), 28(46), pp. 12039-51.

Chouchane S, Girotto S, Yu S, Magliozzo RS. Identification and characterization of tyrosyl radical formation in Mycobacterium tuberculosis catalase-peroxidase (KatG). Journal of Biological Chemistry (2002), 277(45), pp. 42633-38.

Cioni C, Annunziata P. Circulating gp120 alters the blood-brain barrier permeability in HIV-1 gp120 transgenic mice. Neuroscience Letters (2002), 330(3), pp. 299-301.

Clercq ED. Antiviral drug discovery and development: Where chemistry meets with biomedicine. Antiviral Research (2005), 67(2), pp. 56-75.

Collier AC, Helliwell RJ, Tingle MD. 3'-azido-3'-deoxythymidine (AZT) induces apoptosis and alters metabolic enzyme activity in human placenta. Toxicology and Applied Pharmacology (2003), 192, pp. 164-73.

Corasaniti MT. The HIV-1 envelope protein, gp120, causes neuronal apoptosis in the neocortex of the adult rat: a useful experimental model to study neuroaids. Functional Neurology (2001), 16, pp. 31-38.

Cotgreave IA. N-acetylcysteine: pharmacological considerations and experimental and clinical applications. Advanced Pharmacology (1997), 38, pp. 205-227.

Dawson VL, Dawson TM, Synder SH. Human immunodeficiency virus typr 1 coat protein neurotoxicity mediated by nitric oxide in primary cultures. Proceedings of National Academy of Science (1993), 90, pp. 3256-3259.

Do KQ, Trabesinger AH, Kirsten-Kruger M, Lauer C J, Dydak U Hell, Holsboer, F, Boesiger, P, Cuenod M. Schizophrenia: glutathione deficit in cerebrospinal fluid and prefrontal cortex in vivo. European Journal of Neuroscience (2000), 12, pp. 3721–3728.

Dore GJ, Correll PK, Li Y, Kaldor JM, Cooper DA, Brew BJ. Changes to AIDS dementia complex in the era of highly active antiretroviral therapy. AIDS (1999) 13, pp. 1249–1253.

Draper HH, Squires EJ, Mahmoodi H, Wu J, Agarwal M, Hadley M. A comparative evaluation of thiobarbituric acid methods for the determination of malondialdehyde in biological materials. Free Radical Biology Medicine (1993) 15, pp. 353–363.

Droge W Eck HP Mihm S: HIV-induced cysteine deficiency and T-cell dysfunction—a rationale for treatment with N-acetylcysteine. Immunology Today (1992) 13(6), 211-214.

Duke RC, Cohen JJ. Current Protocols Immunology (1999), 1, pp. 1–16.

Estaquier J, Lelièvre JD, Corbeil, J. Effects of Antiretroviral Drugs on Human Immunodeficiency Virus Type 1-Induced CD4$^+$ T-Cell Death. Journal of Virology (2002), 76(12), pp. 5966–5973.

Falchetti A, Franchi A, Martineti V, Tanini A, Brandi ML. Azidothy -midine induces apoptosis and inhibits cell growth and telomerase activity of human parathyroid cancer cells in culture. Journal of Bone and Mineral Research (2005), 20, pp. 410-418.

Fiala, M. TNF-alpha opens a paracellular route for HIV-1 invasion across the blood-brain barrier. Molecular Medicine (1997), 3, pp. 553–564.

Fiala M, Murphy T, MacDougall J, Yang W, Luque A, Arthos J. HAART drugs induce mitochondrial damage and intercellular gaps and gp120 causes apoptosis. Cardiovascular Toxicology (2000), 4, pp. 327-37.

Furuse M, Sasaki H, Tsukita S. Manner of interaction of heterogeneous claudin species within and between tight junction strands. Journal of Cell Biology (1999), 147(4), pp. 891-903.

Gandhi N, Saiyed ZM, Napuri J, Samikkannu T, Reddy PV, Agudelo M, Khatavkar P, Saxena SK, Nair MP. Interactive role of human immunodeficiency virus type 1 (HIV-1) clade-specific Tat protein and cocaine in blood-brain barrier dysfunction: implications for HIV-1-associated neurocognitive disorder. Journa of Neurovirology (2010), 16(4), pp. 294-305.

García-de-la-Asunción J, Gómez-Cambronero LG, Del Olmo ML, Pallardó FV, Sastre J. Viña J. Vitamins C and E prevent AZT-induced leukopenia and loss of cellularity in bone marrow. Studies in mice. Free Radical Research (2007), 41, pp. 330-4.

Gartner S. HIV infection and dementia. Science (2000), 287(5453), pp. 602-4

Gerschenson M, Erhart SW, Paik CY. Poirier MC. Fetal mitochondrial heart and skeletal muscle damage in Erythrocebus patas monkeys exposed in utero to 3'-azido-3'-deoxythymidine. AIDS Research of Human Retroviruses (2000), 16, pp. 635-44.

Giulian D. et al. Study of receptor-mediated neurotoxins released by HIV-1-infected mononuclear phagocytes found in human brain. Journal of Neuroscience (1996), 16, pp. 3139–3153.

Gonda MA. Molecular genetics and structure of the human immunodeficiency virus. Journal of Electron Microscopy and Technology (1988), 1, pp. 17-40.

Gray F, Chrétien F, Vallat-Decouvelaere AV, Scaravilli F. The changing pattern of HIV neuropathology in the HAART era. Journal of Neuropathology and Experimental Neurology (2003), 62(5), pp. 429-40.

Gray F, Bazille C, Adle-Biassette H, Mikol J, Moulignier A, Scaravilli F. Central nervous system immune reconstitution disease in acquired immunodeficiency syndrome patients receiving highly active antiretroviral treatment. Journal of Neurovirology (2005), 113, pp. 16–22.

Green DA. Masliah E, Vinters HV, Beizai P, Moore DJ, Achim CL. Brain deposition of beta-amyloid is a common pathologic feature in HIV positive patients. AIDS (2005), 9, pp. 407-11.

Grieb P. Forster RE, Strome D, Goodwin CW, Pape PC. O2 exchange between blood and brain tissues studied with O2 indicator dilution technique. Journal of Applied Physiology (1985), 58, pp. 1929– 1941.

Grinberg L, Fibach E, Amer J, Atlas D. N-acetylcysteine amide, a novel cell-permeating thiol, restores cellular glutathione and protects human red blood cells from oxidative stress. Free Radical Biology Medicine (2005), 38(1), pp.136-145.

Gu M, Owen AD, Toffa SE, Cooper JM, Dexter D T, Jenner P.Marsden, CD, Schapira, AH. Mitochondrial function,GSH and iron in neurodegeneration and Lewy body diseases. Journal of Neurological Sciences (1998), 158, pp. 24–29.

Halliwell B. Reactive oxygen species in living systems: source, Biochemistry and role in human disease. American Journal of Medicine (1991), pp. 114-122.

Haorah J, Knipe B, Leibhart J, Ghorpade A, Persidsky Y. Alcohol-induced oxidative stress in brain endothelial cells causes blood-brain barrier dysfunction. Journal of Leukocyte Biology (2005), 78, pp. 1223-32.

Holdiness MR.Clinical pharmacokinetics of N-acetylcysteine. Clinical Pharmacokinetics, (1991), 20, pp. 123-134.

Huang CC, Aronstam RS, Chen DR, Huang YW. Oxidative stress calcium homeostasis and altered gene expression in human lung epithelial cells exposed to ZnO nanoparticles. Toxicology *In Vitro* (2010), 1, pp. 45-55.

Ivancich A, Jouve HM, Sartor B, Gaillard J. EPR investigation of compound I in Proteus mirabilis and bovine liver catalases: formation of porphyrin and tyrosyl radical intermediates. Biochemistry (1997), 36(31), pp. 9356-64.

Jiang B, Hebert VY, Li Y, Mathis JM, Alexander JS, Dugas TR. HIV anti retro - viral drug combination induces endothelial mitochondrial dysfunction and reactive oxygen species production but not apoptosis. Toxicology and Applied. Pharmacology (2007), 24, pp. 60-71.

Jochmans D. Novel HIV-1 reverse transcriptase inhibitors. Virus Research (2008), 134(1-2), pp. 171-185.

Kahles T, Luedike P, Endres M, Galla HJ, Steinmetz H, Busse R, Neumann-Haefelin T, Brandes RP. NADPH oxidase plays a central role in blood-brain barrier damage in experimental stroke. Stroke (2007), 38(11), pp. 3000-3006.

Kalams SA, Walker, BD. Cytotoxic T lymphocytes and HIV-1 related neurologic disorders. Current Topics in Microbiology and Immunology (1995), 202, 79–88.

Kasibhatla S. Acridine Orange/Ethidium Bromide (AO/EB) Staining to Detect Apoptosis. Cold Spring Harbor Protocols *(*2006) *pdb*.4493

Kaul M, Garden GA, Lipton SA. Pathways to neuronal injury and apoptosis in HIV-associated dementia. Nature (2001), 410(6831), pp.988-94.

Kaul M. & Lipton SA. Chemokines and activated macrophages in HIV gp120-induced neuronal apoptosis. Proceedings of National Academy of Science (1999), pp. 8212–8216.

Kline ER, Bassit L, Hernandez-Santiago BI, Detorio MA, Liang B, Kleinhenz D, Sutliff RL. Long-term exposure to AZT but not d4T increases endothelial cell oxidative stress and mitochondrial dysfunction. Cardiovascular Toxicology (2009), 1, pp. 1-12.

Knott AB, Perkins G, Schwarzenbacher R, Bossy-Wetzel E. Mitochondrial fragmentation in neurodegeneration. Nature Reviews of Neuroscience, (2008), 9, pp. 505–518.

Kohler JJ, Cucoranu I, Fields E, Green E, He S, Hoying A, Russ R, Abuin A, Johnson D, Hosseini SH, Raper CM, Lewis W. Transgenic mitochondrial superoxide dismutase and mitochondrially targeted catalase prevent antiretroviral-induced oxidative stress and cardiomyopathy. Lab Investigation (2009), 89(7), pp. 782-90

Krebs FC, Ross H, McAllister J, Wigdahl B. HIV-1-associated central nervous system dysfunction. Advanced Pharmacology (2000), 49, pp. 315.

Lemasters JJ, Nieminen AL, Qian T, Trost LC, Elmore SP, Nishimura Y, Crowe RA, Cascio WE, Bradham CA, Brenner DA, Herman B. The mitochondrial permeability transition in cell death: a common mechanism in necrosis, apoptosis and autophagy. Biochimica Biophysics Acta (1998), 1366, pp. 177-96.

Lemasters JJ, Theruvath TP, Zhong Z, Nieminen AL. Mitochondrial calcium and the permeability transition in cell death. Biochimica Biophysics Acta (2009), 1787, pp. 1395–1401.

Lewis W, Dalakas MC. Mitochondrial toxicity of antiviral drugs. Nature Medicine (1995), 1, pp. 417–422.

Lewis W, Gonzalez B, Chromyl A, Paoian. T. Zidovudine induces molecular, bioche mical and ultrastructural changes in rat skeletal muscle mitochondria. Journal of Clinical Investigation (1992), 89, pp.134-1360.
.
Lewis W, Day BJ, Copeland WC. Mitochondrial toxicity of NRTI antiviral drugs: an integrated cellular perspective. Nature Review Drug Discovery (2003), 10, pp. 812-22.

Li Y, Reuter NP, Li X, Liu Q, Zhang J, Martin RC. Colocalization of MnSOD expression in response to oxidative stress. Molecular Carcinogensis (2010), 49(1), pp. 44-53.

Lichtner M, Mengoni F, Mastroianni CM, Sauzullo I, Rossi R, De Nicola M, Ghibelli L. HIV protease inhibitor therapy reverses neutrophil apoptosis in AIDS patients by direct calpain inhibition. Apoptosis (2006), 11, pp. 781-7.

Lin MT, Beal MF. Mitochondrial dysfunction and oxidative stress in neurodegenerative diseases. Nature (2006), 443, pp. 787–795.

Lipton SA, Gendelman HE. Dementia associated with the acquired immunodeficiency syndrome. New England Journal of Medicine, (1995), 332, pp. 934–940.

Liu JH, Chen MM, Huang JW, Wann H, Chao HM. Therapeutic effects and mechanisms of action of mannitol during H2O2-induced oxidative stress in human retinal pigment epithelium cells. Journal of Ocular Pharmacology and Therapeutics (2010), 26(3), pp. 249-57.

Mallon PW Unemori P Sedwell R Morey A Rafferty M Williams K Chisholm D Samaras K, Emery S, Kelleher A, Cooper DA, Carr A. In vivo nucleoside reverse-transcriptase inhibitor salter expression of both mitochondrial and lipid metabolism genes in the absence of depletion of mitochondrial DNA. Journal of Infection Disinfectants (2005), 191, pp.1686–1696.

Marnett LJ. Lipid peroxidation-DNA damage by malondialdehyde. Mutation Research (1999), 424, pp. 83–95.

Mattson DM, Ahmad IM, Dayal D, Parsons AD, Aykin-Burns N, Li L, Orcutt K, P. Spitz DR, Dornfeld KJ, Simons AL. Cisplatin combined with zidovudine enhances cytotoxicity and oxidative stress in human head and neck cancer cells via a thiol-dependent mechanism. Free Radical Biology and Medicine (2009), 46, pp. 232-237.

McArthur JC. HIV dementia an evolving disease. Journal of Neuroimmunology (2004), 157(1-2), pp. 3-10.

Meister A. Glutathione metabolism. Methods in Enzymology (1995), 251, pp. 3–7.

Minagar A, Alexander JS. Blood-brain barrier disruption in multiple sclerosis. Multiplie. Sclerosis (2003), 9, pp. 540-549.

Mondal D, Pradhan L, Ali M, Agrawal KC. HAART drugs induce oxidative stress in human endothelial cells and increase endothelial recruitment of mononuclear cells pp. exacerbation by inflammatory cytokines and amelioration by antioxidants. Cardiovascular Toxicology (1999), 4, pp. 287-302.

Monini P   Sgadari C Barillari S   Ensoli B. HIV protease inhibitors pp. antiretroviral agents with anti-inflammatory anti-angiogenic and anti-tumour activity. Journal of Antimicrobial Chemotherapy (2003), 51, pp. 207–211.

Mueller SG, Trabesinger AH,   Boesiger P, Wieser HG. Brain glutathione levels in patients with epilepsy measured by in vivo 1H-MRS. Neurology (2001), 57, pp. 1422–1427.

Nath A. Human immunodeficiency virus (HIV) proteins in neuropathogenesis of HIV dementia. Journal of Infectious Diseases (2002), 186, pp. S193

Navia BA, Cho ES, Petito CK, Price RW. The AIDS dementia complex pp. II. Neuropathology. Annals of Neurology (1983), 19, pp. 525–535.

Neal R. Matthews RH. Lutz P. Ercal N.   Antioxidant role of N-acetyl cysteine isomers following high dose irradiation. Free Radical Biology Medicine (2003), 34(6), pp. 689-695.

O'Brien WJ, Heimann T, Rizvi F. NADPH oxidase expression and production of superoxide by human corneal stromal cells. Molecular Vision (2009), 15, pp. 2535-43.

Offen D, Gilgun-Sherki Y, Barhum Y, Benhar M, Grinberg L, Reich R, Melamed E Atlas D. A low molecular weight copper chelator crosses the blood-brain barrier and attenuates experimental autoimmune encephalomyelitis. Journal of Neurochemistry (2004), 89, pp. 1241-1251.

Oiry J, Mialocq P, Puy JY, Fretier P, Dereuddre-Bosquet N, Dormont D, Imbach JL Clayette P pp. Synthesis and biological evaluation in human monocyte-derived macrophages of N-(N-acetyl-L-cysteinyl)-S-acetylcysteamine analogues with potent antioxidant and anti-HIV activities. Journal of Medicinal Chemistry (2004), 47(7), pp.1789-1795.

Opii WO, Sultana R, Abdul HM, Ansari MA, Nath A, Butterfield DA. Oxidative stress and toxicity induced by the nucleoside reverse transcriptase inhibitor (NRTI)-2′ 3′-dideoxycytidine (DDC) : relevance to HIV-dementia. Experimental Neurology (2007), 204, pp. 29–38.

Pan W, Kastin AJ. Changing the chemokine gradientpp. CINC1 crosses the blood-brain barrier. Journal of Neuroimmunology (2001), 115(1-2), pp. 64-70.

Pardridge WM. Brain metabolism: a perspective from the bloodbrain barrier. Physiology Reviews (1983), pp. 1481–1535.

Penugonda S, Mare S, Goldstein G, Banks WA, Ercal N. Effects of N-acetylcysteine amide (NACA), a novel thiol antioxidant against glutamate-induced cytotoxicity in neuronal cell line PC12. Brain Research (2005), 1056(2), pp. 132-8.

Petito CK, Cash KS. Blood-brain barrier abnormalities in the acquired immune deficiency syndrome immunohistochemical localization of serum proteins in postmortem brain. Annals of Neurology (1992), 32, pp. 658-666.

Piacentini M, Kroemer G. Cell death pathways in retroviral infection. Cell Death Differentiation, (2005), S1, pp. 835-6.

Pinton P, Giorgi C, Siviero R, Zecchini E, Rizzuto R. Calcium and apoptosis: ER-mitochondria Ca^{2+} transfer in the control of apoptosis. Oncogene (2008), 27(50), PP. 6407-18.

Pocernich CB, Fontaine M, Butterfield DA. In vivo glutathione elevation protects against hydroxyl free radical-induced protein oxidation in rat brain. Neurochemistry International (2000), 36, pp. 185-191.

Power C, Kong PA, Crawford TO, Wesselingh S, Glass JD, McArthur JC, Trapp BD. Cerebral white matter changes in acquired immunodeficiency syndrome dementia : alteration of the blood–brain barrier. Annals of Neurology (1993), 34, pp. 339–350.

Price TO, Uras F, Banks WA, Ercal N. A novel antioxidant N-acetylcysteine amide prevents gp120- and Tat-induced oxidative stress in brain endothelial cells. Experimental Neurology (2006), 201, pp. 193-202.

Prospéro-García O, Gold LH, Fox HS, Polis I, Koob GF, Bloom FE, Henriksen SJ. Microglia-passaged simian immunodeficiency virus induces neurophysiological abnormalities in monkeys. Proceedings in National Academy of Sciences (1996), 93(24), pp. 14158-14163.

Quijano C, Alvarez B, Gatti RM, Augusto O, Radi R. Pathways of peroxynitrite oxidation of thiol groups. Biochemistry Journal (1997), 322 (Pt 1), pp.167-173.

Robertson KR, Su Z, Margolis DM, Krambrink A, Havlir DV, Evans S, Skiest DJ. Neurocognitive effects of treatment interruption in stable HIV-positive patients in an observational cohort. Neurology (2010), 74, pp. 1260-6.

Rumbaugh JA, Nath A. Developments in HIV neuropathogenesis. Current Pharmaceutical Design (2006), 12, pp. 1023–1044.

Sankarapandi S, Zweier JL, Mukherjee G, Quinn MT, Huso DL. Measurementand characterization of superoxide generation in microglial cells: evidence for an NADPH oxidase-dependent pathway. Archive of Biochemistry and Biophysics (1998), 353, pp. 312–321.

Sacktor N, McDermott MP, Marder K, Schifitto G, Selnes OA, McArthur JC, Cohen B, Epstein L. HIV-associated cognitive impairment before and after the advent of combination therapy. Journal of Neurovirology (2002), 8, pp.136–142.

Sandoval R, Malik AB, Minshall RD, Kouklis P, Ellis CA, Tiruppathi C. Ca(2+) signalling and PKC alpha activate increased endothelial permeability by disassembly disassembly of VE-cadherin junctions. Journal of Physiology (2001), 1, pp. 433-45.

Schweinsburg BC, Taylor MJ, Alhassoon OM, Gonzalez R, Brown GG, Ellis RJ, Letendre S, Videen JS, McCutchan JA, Patterson TL, Grant I. Brain mitochondrial injury in human immunodeficiencyvirus-seropositive (HIV+) individuals taking nucleoside reverse transcriptase inhibitors. Journal of Neurovirology (2005), 11, pp. 356–364.

Scott GS, Virág L, Szabó C, Hooper DC. Peroxynitrite-induced oligodendrocyte toxicity is not dependent on poly (ADP-ribose) polymerase activation. Glia (2003), 41(2), pp.105-16.

Shi R, Huang CC, Aronstam RS, Ercal N, Martin A, Huang YW. N-acetylcysteine amide decreases oxidative stress but not cell death induced by doxorubicin in H9c2 cardiomyocytes. BMC Pharmacology (2009), 9, pp. 1-9.

Simpson MV, Chin CD, Keilbaugh SA, Lin, TS, Prusoff WH. Studies on the inhibition of mitochondrial DNA replication by 3'-azido-3'-deoxythymidine and other dideoxynucleoside analogs which inhibit HIV-1 replication. Biochemical Pharmacology (1989), 38, pp.1033-6.

Skulachev VP. Cytochrome c in the apoptotic and antioxidant cascades. FEBS Letters (1998), 423, pp. 275-80.

Sonnerborg A, Carlin G, Akerlund B, Jarstrand C. Increased production of malondialdehyde in patients with HIV infection. Scandnavian Journal of Infectious Disinfectant (1998), 20, pp. 287–290.

Staal FJ, Roederer M, Herzenberg LA, Herzenberg LA. Intracellular thiols regulate activation of nuclear factor kappa B and transcription of human immunodeficiency virus. Proceedings of National Academy of Science (1990), 87(24), pp. 9943-9947.

St'astný F, Skultétyová I, Pliss L, Jezová D. Quinolinic acid enhances permeability of rat brain microvessels to plasma albumin. Brain Research Bulletin (2000), 53(4), pp. 415-420.

Stéphanie V, Franck T, Régis R. Nelfinavir induces necrosis of 3T3F44-2A adipocytes by oxidative Stress. Journal of Acquired Immune Deficiency Syndrome (2004), 37(5), pp. 1556-1562.

Suarez J, Ranguelova K, Jarzecki AA, Manzerova J, Krymov V, Zhao X, Yu S, Metlitsky L, Gerfen G J, Magliozzo RS. An oxyferrous heme/protein-based radical intermediate is catalytically competent in the catalase reaction of Mycobacterium tuberculosis catalase-peroxidase (KatG). Journal of Biological Chemistry (2009), 284, pp.7017-7029.

Szabados E, Fischer GM, Toth K, Csete B, Nemeti B, Trombitas K, Habon T, Endrei D, Sumegi B. Role of reactive oxygen species and poly-ADP-ribose polymerase in the development of AZT-induced cardiomyopathy in rat. Free Radical Biology Medicine (1999), 3-4, pp. 309-17.

Taylor DE, Ghio AJ, Piantadosi CA. Reactive oxygen species produced by liver mitochondria of rats in sepsis. Archives in Biochemistry and Biophysics (1995), 316, pp. 70-76.

Toborek M, Lee YW, Pu H, Malecki A, Flora G, Garrido R, Hennig B, Bauer HC, Nath A. HIV-Tat protein induces oxidative and inflammatory pathways in brain endothelium. Journal of Neurochemistry (2003), 84(1), pp. 169-179.
.

Toborek M, Lee YW, Flora G, Pu H, András IE, Wylegala E, Hennig B, Nath A. Mechanisms of the blood-brain barrier disruption in HIV-1 infection. Cellular and Molecular Neurobiology (2005), 25(1), pp. 181-199.

Toneatto S, Finco O, van der Putten H, Abrignani S, Annunziata P. Evidence of blood-brainbarrier alteration and activation in HIV-1 gp120 transgenic mice. AIDS (1999), 13, pp. 2343–2348.
.

Turchan J, Pocernich CB, Gairola C, Chauhan A, Schifitto G, Butterfield DA, Buch S Narayan O, Sinai A, Geiger J, Berger JR, Elford H, Nath A. Oxidative stress in HIV demented patients and protection ex vivo with novel antioxidants. Neurology (2003), 60, pp.307–314.

Vincent S, Tourniaire F, El Yazidi CM, Compe E, Manches O, Plannels R, Roche R. Nelfinavir induces necrosis of 3T3F44-2A adipocytes by oxidative stress. Journal of Acquired Immune Deficiency Syndrome, (2004), 37(5), pp. 1556-62.

Wang H, Joseph JA. Quantifying cellular oxidative stress by dichlorofluorescein assay using microplate reader. Free Radical Biology and Medicine (1999), 5-6, pp. 612-6.

Wang X, Chai H, Lin PH, Yao Q, Chen C. Roles and mechanisms of human immunodeficiency virus protease inhibitor ritonavir and other anti-human immunodeficiency virus drugs in endothelial dysfunction of porcine pulmonary arteries and human pulmonary artery endothelial cells. American Journal of Pathology (2009), 174(3), pp.771-81.

Whitmer RA, Sidney S, Selby J, Johnston SC, Yaffe K. Midlife cardiovascular risk factors and risk of dementia in late life. Neurology (2005), 64, pp.277–281.

Winters R, Zukowski J, Ercal N, Matthews D, Spitz DR. Analysis of glutathione, glutathione disulphide, cysteine, homocysteine and other biological thiols by HPLC following derivatization with N-(1-pyrenyl) malemide. Analytical Biochemistry (1995), 227, pp.14-21.

Woods SP, Moore DJ, Weber E, Grant I. Cognitive neuropsychology of HIV-associated neurocognitive disorders. Neuropsychological Reviews (2009), 19(2), pp. 152-68.

Wu Z, Florence M, Hofman S, Zlokovic BV. A simple method for isolation and characterization of mouse brain microvascular endothelial cells. Journal of Neuroscience methods (2003),130(1), pp 53-63.

Xiang S, Pan W. Strategies to create a regenerating environment for the injured spinal cord. Current Pharmaceutical Design (2005), 11, pp. 1267-1277.

Xu J, Ikezu T. The comorbidity of HIV-associated neurocognitive disorders and Alzheimer's disease a foreseeable medical challenge in post-HAART era. Journal of Neuroimmune Pharmacology (2009), 4(2), pp. 200-12.

Yeni PG, Hammer SM, Hirsch MS, Saag MS, Schechter M, Carpenter BCC, Fischl MA, Gatell JM, Gazzard BG, Jacobsen DM, Katzenstein DA, Montaner JS, Richman DD, Schooley RT, Thompson MA, Vella S, Volberding PA. Treatment for adult HIV infection : recommendations of the International AIDS Society-USA Panel. JAMA (2004), 292, pp. 251–265.

Zhang X, Banerjee A, Banks WA, Ercal N. N-Acetylcysteine amide protects against methamphetamine-induced oxidative stress and neurotoxicity in immortalized human brain endothelial cells. Brain Research (2009), 1275, pp.87-95.

Zhang H, Xu Y, Joseph J, Kalyanaraman B. Intramolecular electron transfer between tyrosyl radical and cysteine residue inhibits tyrosine nitration and induces thiyl radical formation in model peptides treated with myeloperoxidase, H2O2, and NO2-: EPR SPIN trapping studies. Journal of Biological Chemistry (2005), 280(49), pp. 40684-98.

Zipser BD, Johanson CE, Gonzalez L, Berzin TM, Tavares R. Hulette CM. Vitek MP, Hovanesian V. Stopa EG. Microvascular injury and blood-brain barrier leakage in Alzheimer's disease. Neurobiology of. Aging (2007), 28, pp. 977-986.

Zoccali C, Mallamaci F, Tripepi G. AGE's and carbonyl stress pp. potential pathogenic factors of long-term ureamic complications. Nephrology and Dialysis Transplant (2000), 15, pp. S7-10.

VITA

Kalyan Chakravarthy Reddy Manda was born on January 8, 1978 in Kavitam, India. He obtained his primary and secondary education in Guntakal, India and he received his Bachelor of Pharmacy in June, 2002. From the spring of 2003 to the fall 2004, he was enrolled in the Chemistry Department in Missouri University of Science and Technology (Missouri S&T) in Rolla, MO and he received a Master of Science Degree in December 2008. He enrolled as a PhD student at Missouri S&T in fall 2004 and began his doctoral studies at that time.